nature ecology & evolution

SUPPLEMENTARY INFORMATION

DOI: 10.1038/s41559-017-0297-1

In the format provided by the authors and unedited.

Corrected: Author correction

Intermediate degrees of synergistic pleiotropy drive adaptive evolution in ecological time

Léa Frachon[1], Cyril Libourel[1], Romain Villoutreix[2], Sébastien Carrère[1], Cédric Glorieux[2], Carine Huard-Chauveau[1], Miguel Navascués[3,4], Laurène Gay[5], Renaud Vitalis[3,4], Etienne Baron[2], Laurent Amsellem[2], Olivier Bouchez[6,7], Marie Vidal[6,8], Valérie Le Corre[9], Dominique Roby[1], Joy Bergelson[10] and Fabrice Roux[1,2]*

[1]LIPM, Université de Toulouse, INRA, CNRS, 31326 Castanet-Tolosan, France. [2]Laboratoire Evolution, Ecologie et Paléontologie, UMR CNRS 8198, Université de Lille, 59655 Villeneuve d'Ascq Cedex, France. [3]INRA, UMR CBGP, 34988 Montferrier-sur-Lez, France. [4]Institut de Biologie Computationnelle, Montpellier 34095, France. [5]UMR AGAP, INRA, 34060 Montpellier, France. [6]INRA, GeT-PlaGe, Genotoul, 31326 Castanet-Tolosan, France. [7]GenPhySE, Université de Toulouse, INRA, INPT, INP-ENVT, 31326 Castanet-Tolosan, France. [8]INRA, UAR1209, 31326 Castanet-Tolosan, France. [9]INRA, UMR1347, Agroécologie, 21065 Dijon, France. [10]Department of Ecology and Evolution, University of Chicago, Chicago, IL 60637, USA.
Léa Frachon and Cyril Libourel contributed equally to this work. *e-mail: fabrice.roux@inra.fr

nature ecology & evolution

SUPPLEMENTARY INFORMATION

DOI: 10.1038/s41559-017-0297-1

In the format provided by the authors and unedited.

Intermediate degrees of synergistic pleiotropy drive adaptive evolution in ecological time

Léa Frachon[1], Cyril Libourel[1], Romain Villoutreix[2], Sébastien Carrère[1], Cédric Glorieux[2], Carine Huard-Chauveau[1], Miguel Navascués[3,4], Laurène Gay[5], Renaud Vitalis[3,4], Etienne Baron[2], Laurent Amsellem[2], Olivier Bouchez[6,7], Marie Vidal[6,8], Valérie Le Corre[9], Dominique Roby[1], Joy Bergelson[10] and Fabrice Roux[1,2]*

[1]LIPM, Université de Toulouse, INRA, CNRS, 31326 Castanet-Tolosan, France. [2]Laboratoire Evolution, Ecologie et Paléontologie, UMR CNRS 8198, Université de Lille, 59655 Villeneuve d'Ascq Cedex, France. [3]INRA, UMR CBGP, 34988 Montferrier-sur-Lez, France. [4]Institut de Biologie Computationnelle, Montpellier 34095, France. [5]UMR AGAP, INRA, 34060 Montpellier, France. [6]INRA, GeT-PlaGe, Genotoul, 31326 Castanet-Tolosan, France. [7]GenPhySE, Université de Toulouse, INRA, INPT, INP-ENVT, 31326 Castanet-Tolosan, France. [8]INRA, UAR1209, 31326 Castanet-Tolosan, France. [9]INRA, UMR1347, Agroécologie, 21065 Dijon, France. [10]Department of Ecology and Evolution, University of Chicago, Chicago, IL 60637, USA.
Léa Frachon and Cyril Libourel contributed equally to this work. *e-mail: fabrice.roux@inra.fr

SUPPLEMENTARY METHODS

Plant material

In this study, we focused on the population TOU-A located under a 350m electric fence separating two permanent meadows experiencing cycles of periodic grazing by cattle (**Supplementary Fig. 1A**) in the village of Toulon-sur-Arroux (Burgundy, East of France, N 46°38'57.302'', E 4°7'16.892''). Seeds from individual plants were collected in 2002 (TOU-A1), 2007 (TOU-A5) and 2010 (TOU-A6) according to a sampling scheme allowing us to take into account the density of *A. thaliana* plants along the transect: (1) from the starting point of the transect (**Supplementary Fig. 1A**), walk along the transect until a plant is found and collect seeds from this plant, (2) if this plant is at the beginning of a patch, then collect seeds from plants located every 50 cm along this patch, (3) else, walk along the transect until a new plant is found and collect seeds from this plant. According to this sampling scheme, seeds of 80, 115 and 115 individual plants were collected in 2002, 2007 and 2010, respectively (**Supplementary Fig. 1**). Seeds collected from those 310 individual plants constitute seed families, hereafter named accessions. Given the outcrossing rate of ~6% observed in the TOU-A population[1], the 310 accessions were considered as relatively homozygous across the genome.

Seeds from the 80 accessions collected in 2002 were grown individually in a controlled greenhouse at The University of Chicago (USA) and seeds for each TOU-A1 accession collected. The analysis of these 80 accessions genotyped at 149 SNPs gave an estimate of selfing rate of ~94%[1].

Differences in the maternal effects among the 310 accessions were reduced by growing one plant of each family for one generation under controlled greenhouse conditions (16-h photoperiod, 20°C) in early 2011 at the University of Lille 1. For this purpose, we planted seeds produced at The University of Chicago for accessions from the TOU-A1 population, and seeds collected in the field for accessions from the TOU-A5 and TOU-A6 populations. For the purpose of this study, we only used seeds from the 80 accessions collected in 2002 and from the 115 accessions collected in 2010.

Ecological characterization

Climate characterization

Data for the mean annual temperature, the mean warmest month temperature, the mean coldest month temperature, the sum of degree-days above 5°C, the sum of degree-days below 0°C and the mean annual precipitation were retrieved from 1970 to 2013. Climate data was generated with the ClimateEU v4.63 softwarepackage, available at *http://tinyurl.com/ClimateEU*, based on methodology described in Hamann *et al.* (2013)[2].

Soil characterization

A sample of the 5-cm upper soil layer was collected at 83 positions scattered along the transect in 2010 (**Supplementary Fig. 1**). These samples were air-dried in the greenhouse (20-22°C), and then stored at room temperature. As described in Brachi *et al.*(2013)[3], each soil

sample was characterized for 14 edaphic factors: pH, maximal water holding capacity (WHC), total nitrogen content (N), organic carbon content (C), C/N ratio, soil organic matter content (SOM), concentrations of P_2O_5, K, Ca, Mg, Mn, Al, Na and Fe. Iron concentration (Fe) was excluded from further analyses due to a lack of variation among the 83 samples. In order to reduce multicollinearity, the set of remaining 13 edaphic variables was pruned based on the pairwise Spearman correlations of the variables, so that no two variables had a Spearman *rho* greater than 0.8. In cases where variables were strongly inter-correlated, we selected the one with the most obvious link to the ecology of *A. thaliana*. The final set of 10 edaphic variables considered in this study was N, C/N ratio, pH, WHC, P_2O_5, K, Mg, Mn, Na and Al.

To visualize the edaphic space of the TOU-A population, we conducted a principal component analysis (PCA) based on the 83 values of the 10 edaphic traits (*R* package ade4)[4].

Phenotypic characterization

Experimental design

An experiment of 5850 plants was set up at the local site of the TOU-A population. The experimental design and the experimental conditions are illustrated on **Supplementary Fig. 1**. Based on the edaphic space (**Supplementary Fig. 3**), we defined three contrasting edaphic areas under the electric fence, hereafter named soil types A, B and C. In late August 2012, a 12.3-m² (4.4m * 2.8) plot was delimited by an electric fence for protection against cattle in each soil type. In each plot, one subplot of 2.88-m² (4.8m * 0.6m, experimental condition without the presence of *P. annua*, see below) and one subplot of 3.36-m² (4.8m * 0.7m, experimental condition with the presence of *P. annua*, see below) were arranged at 80-cm spacing. In late August 2012, each subplot was manually weeded and tilled for the 10-cm upper soil layer. The 24th of September 2012, subplots were surrounded by green plastic covers for weed control. To mimic the main natural germination cohort observed in the TOU-A population in late September 2012 (**Supplementary Fig. 1**), seeds were sown on the 24th of September 2012 for the experimental conditions 'soil A without *P. annua*', ''soil A with *P. annua*' and 'soil B without *P. annua*', and on the 25th of September 2012 for the experimental conditions 'soil B with *P. annua*', ''soil C without *P. annua*' and 'soil C with *P. annua*'. Each of the six *in situ* experimental conditions was organized in five blocks, each one being represented by 3 arrays of 66 individual wells (Ø4 cm, vol. ~38 cm^3) (TEKU, JP 3050/66). Across the five blocks, the 15 arrays were stuck some on the others and organized according to a grid of 15 columns and one line. To buffer against possible border effects in the experimental conditions with *P. annua*, the 15 arrays were surrounded by one row of wells sown with both *P. annua* and *A. thaliana* (accession TOU-A6-69 collected in 2010). All the wells were first filled with 3 cm of the respective native soil, then with an additional 1cm of the respective native soil that was oven dried for two days at 65°C. The oven dried native soil prevented germination from the seed bank, whereas the 3-cm native soil allowed the colonization of the oven dried native soil by native microbiota.

In each of the six *in situ* experimental conditions, each of the five blocks corresponded to an independent randomization of 195 plants with one replicate per accession collected in

2002 and 2010. In each block, the remaining three wells were left empty. Five seeds of *A. thaliana* were sown in each well. For the three *in situ* experimental conditions with *P. annua*, a mean number of five seeds of *P. annua* were additionally sown in each well. Seeds for *P. annua* were ordered to the company Herbiseeds (http://www.herbiseed.com/home.aspx). After sowing, arrays were directly transported *in situ* and slightly buried in their dedicated soil types. Arrays were covered for 10 days with an agricultural fleece that allowed the seeds to be exposed to rain and sunlight while preventing them from disturbance by rain drops.

Germination date was monitored daily for 10 days (see below). Seeds germinated in more than 97.74 % of the wells. Wells were thinned to one seedling of *A. thaliana* and/or one seedling of *P. annua* between 18 and 22 days after sowing. During the course of the experiment (late September 2012 – late June 2013), plants were protected from herbivory by slugs as described in Brachi *et al.* (2010)[5].

Measured traits

Each plant was scored for a total of 29 phenotypic traits related to phenology (n = 4), resource acquisition (n = 1), architecture and seed dispersal (n = 9), fecundity (n = 14) and survival (n = 1). These traits were chosen to characterize the life history of *A. thaliana* including the timing of offspring production or seed dispersal[3,6-8], or because they are involved in the response to competition[9,10], and/or are good estimators of life-time fitness and reproductive strategies[7,11-14]. Most of these traits have been fully described in Roux *et al.* (2016)[14]:

- *Phenology*: Germination time (GERM) was measured as the number of days between sowing and the emergence of the first seedling (opening of both cotyledons). Bolting time (BT), flowering interval (INT) and the reproductive period (RP) were scored as the interval between germination date and bolting date (inflorescence distinguishable from the leaves at a size < 5 mm), between bolting date and flowering date (appearance of the first open flower) and between flowering date and date of maturation of the last fruit, respectively.
- *Resource acquisition*: At the start of flowering, the maximum diameter of the rosette measured to the nearest millimeter was used as a proxy for plant size (DIAM).
- *Architecture and seed dispersal*: After maturation of the last fruit, the above-ground portion was harvested and stored at room temperature. Plants were later phenotyped for the following architectural and seed dispersal related traits: height from soil to the first fruit on the main stem (H1F, in mm), height of the main stem (HSTEM, in mm), maximum height (HMAX, in mm), number of primary branches on the main stem with fruits (RAMPB_WF) or without fruits (RAMPB_WOF), total number of primary branches (TOTPB), total number of basal branches (RAMBB) and total number of branches (TOTB = TOTPB + RAMBB). We also evaluated a response strategy to competition (ratio HD = H1F / DIAM)[9].
- *Fecundity*: Because the number of seeds in a fruit is highly correlated with fruit length[11], total seed production was approximated by total fruit length (FITTOT, in mm). Seed production is a good proxy for fecundity in a highly selfing annual species like *A. thaliana*. FITTOT was obtained by adding the fruit length produced on the main stem

(FITSTEM, in mm), the primary branches on the main stem (FITPB, mm) and the basal branches (FITBB, in mm). These estimates of fruit length were obtained by counting the number of fertilized fruits produced on each type of branches (FRUITSTEM, FRUITPB and FRUITBB) and multiplying these counts by an estimate of their corresponding fruit (or silique) length (SILSTEM, SILPB and SILBB, in mm), estimated as the average of three haphazardly selected representative fruits. We also calculated three ratios corresponding to the percentage of seeds produced by one branch type as a function of the total amount of seed produced: RSTEM = FITSTEM / FITTOT, RPB = FITPB / FITTOT and RBB = FITBB / FITTOT. Finally, we estimated the average length between two fruits on the main stem (INTERNOD = (HSTEM – H1F) / (FRUITSTEM - 1); in mm).

- *Survival*: All plants that germinated but did not survive were counted as dead (SURVIVAL = 0). Harvested plants were counted as alive (SURVIVAL = 1).

Genomic characterization

DNA extraction, libraries preparation and genome sequencing

Genomic DNA for the 195 accessions collected in 2002 and 2010 was extracted as described in Brachi *et al.* (2013)[3]. DNAseq was performed at the GeT-PlaGe core facility (INRA Toulouse). DNA-seq libraries were prepared according to Illumina's protocol using the Illumina TruSeq Nano LT Kit. Briefly, DNA was fragmented by sonication on a covaris M220, size selection was performed using CLEANNA CleanPCR beads and adaptators were ligated for sequencing. Library quality was assessed using an Advanced Analytical Fragment Analyser and libraries were quantified by QPCR using the Kapa Library Quantification Kit. DNA-seq experiments were performed on an Illumina HiSeq2500 using a paired-end read length of 2x100 pb with the Illumina TruSeq SBS v3 Reagent Kits. Each PCR product with tag-sequence was first quantified using PicoGreen® dsDNA Quantitation Reagent. Then a mix was made depending on these quantities in order to obtain an equimolar pool.

Mapping and SNP calling

Raw reads of each of the 195 accessions were mapped onto the *A. thaliana* reference genome Col-0 (genome size: 119Mb, TAIR10, https://www.arabidopsis.org/portals/genAnnotation/gene_structural_annotation/annotation_data.jsp) using glint software (1.0.rc8; Faraut & Courcelle, unpublished software) with the following parameters: a maximum of 5 mismatches on at least 80 nucleotides and keep alignments with the best score (*glint mappe --no-lc-filtering --best-score --mmis 5 --lmin 80 --step 2*). The mapped reads were filtered for proper pairs with SAMtools (v0.01.19)[15] (*samtools view -f 0x02*). The mean and the median coverage to a unique position in the reference genome was ~25.5x and ~24.5x, respectively.

A stringent SNPCalling across the genome was then performed for each accession with SAMtools mpileup (v0.01019)[15] and VarScan (v2.3)[16] with the parameters corresponding to a theoretical sequencing coverage of 30X and the search for homozygous sites (*samtools mpileup -B ; VarScan mpileup2snp --min-coverage 5 --min-reads2 4 --min-avg-qual 30 --min-var-freq*

0.97 --p-value 0.01). Due to the relatively high selfing rate observed in *A. thaliana* and the generation(s) of selfing performed in greenhouse conditions (see the subsection 'Plant material'), the frequency of heterozygous sites should be low; those sites were not considered in this study in order to avoid paralogs. All polymorphic sites were then identified among the 195 accessions. Finally, a SNP calling based on all accessions was performed on all polymorphic sites to differentiate null values from the reference value. Sites with more than 50% missing values were discarded from the set of polymorphic sites.

Testing whether the mean Linkage Disequilibrium extent in the TOU-A population is short enough for fine mapping of genomic regions associated with natural phenotypic variation

The presence of significant associations at loci known to be involved in well described phenotypes provides a proof-of-concept for the power of conducting GWAS in a given mapping population. To estimate the power of fine mapping in the TOU-A population, we focused (i) on the *R* genes *RPM1* and *RPS2* responsible for the hypersensitive cell death response (HR) against the engineered bacterial strain of *Pseudomonas syringae* DC3000 expressing either *AvrRpm1* (DC3000::AvrRpm1) or *AvrRpt2* (DC3000::AvrRpt2), respectively, and (ii) on the atypical kinase *RKS1* conferring quantitative broad-spectrum resistance against the vascular bacterial pathogen *Xanthomonas campestris* pv. *campestris* (reviewed in Roux & Bergelson (2016)[17]). The 195 accessions collected in 2002 and 2010 were grown, inoculated and phenotyped for (i) qualitative resistance against DC3000::AvrRpm1 (leaf collapse scored at 6hpi) and DC3000::AvrRpt2 (leaf collapse scored at 1dpi) as described in Vailleau *et al.* (2002)[18], and (ii) quantitative resistance against the strain *Xcc568* (disease index scored using a scale from 0 to 4 at 10dpi) as described in Huard-Chauveau *et al.* (2013)[19]. Given the broad-sense heritability values close to one observed for qualitative resistance[20], four leaves of a single plant were inoculated for each accession. For quantitative resistance against *Xcc568*, a randomized complete block design was set up with two blocks, each being an independent randomization of one replicate per accession. In the latter case, the following general linear model was used to analyze disease index (GLM procedure in SAS9.1, SAS Institute Inc., Cary, North Carolina, USA):

$$\text{disease index}_{ij} = \mu + \text{block}_i + \text{accession}_j + \varepsilon_{ij}$$

where 'μ' is the overall mean; 'block' accounts for differences among the two experimental blocks; 'accession' corresponds to the 195 natural accessions; and 'ε' is the residual term. Normality of the residuals was not improved by transformation of the data. Least-square mean (LSmean) was obtained for each natural accession

GWA mapping was run using a mixed-model approach implemented in the software EMMAX (Efficient Mixed-Model Association eXpedited)[21]. This model includes a genetic kinship matrix as a covariate to control for population structure.GWA mapping was based on (i) raw means for qualitative resistance against DC3000::AvrRpm1 and DC3000::AvrRpt2, and (ii) LSmeans for quantitative resistance against *Xcc568*.

References to Supplementary Information

1. Platt, A. *et al.* The scale of population structure in *Arabidopsis thaliana*. *PLoS Genet.* **6**, e1000843 (2010).
2. Hamann, A., Wang**,** T., Spittlehouse, D.L. & Murdock, T.Q. A comprehensive, high-resolution database of historical and projected climate surfaces for western North America. B. Am. Meteorol. Soc. **94**, 1307 (2013).
3. Brachi, B. *et al.* Investigation of the geographical scale of adaptive phenological variation and its underlying genetics in *Arabidopsis thaliana*. *Mol. Ecol.* **22**, 4222-4240 (2013).
4. Chessel, C., Dufour, A.B. & Thioulouse, J. The ade4 package – I – One-table methods. *R News* **4**, 5 (2004).
5. Brachi, B. *et al.* Linkage and association mapping of *Arabidopsis thaliana* flowering time in nature. *PLoS Genet.* 6:e1000940 (2010).
6. Weinig, C. *et al.* Novel loci control variation in reproductive timing in *Arabidopsis thaliana* in natural environments. *Genetics* **162**, 1875-1884 (2002).
7. Reboud, C. *et al.* Natural variation among accessions of *Arabidopsis thaliana*: beyond the flowering date, what morphological traits are relevant to study adaptation? In Plant adaptation: molecular biology and ecology. Edited by Q. C. Cronk, J. Whitton and I. Taylor. NRC Research Press, Ottawa, Canada. pp 135-142 (2004).
8. Wender, N.J., Polisetty, C.R. & Donohue, K. Density-dependent processes influencing the evolutionary dynamics of dispersal: a functional analysis of seed dispersal in *Arabidopsis thaliana* (Brassicaceae). *Am. J. Bot.* **92**, 960-971 (2005).
9. Baron, E., Richirt, J., Villoutreix, R., Amsellem, L. & Roux, F. The genetics of intra- and interspecific competitive response and effect in a local population of an annual plant species. *Funct. Ecol.* **29**, 1361-1370 (2015).
10. Brachi, B., Aimé, C., Glorieux, C., Cuguen, J. & Roux, F. Adaptive value of phenological traits in stressful environments: predictions based on seed production and Laboratory Natural Selection. *PLoS One* **7**, e32069 (2012).
11. Roux, F., Gasquez, J. & Reboud, X. The dominance of the herbicide resistant cost in several *Arabidopsis thaliana* mutant lines. *Genetics* **166**, 449-460 (2004).
12. Roux, F., Giancola, S., Durand, S. & Reboud, X. Building of an experimental cline with *Arabidopsis thaliana* to estimate herbicide fitness cost. *Genetics* **173**,1023-1031 (2006).
13. Bac-Molenaar, J.A. *et al.* Genome-wide association mapping of fertility reduction upon heat stress reveals developmental stage-specific QTLs in *Arabidopsis thaliana*. *The Plant Cell* **27**, 1857-1874 (2015).
14. Roux, F. *et al.* Cytonuclear interactions affect adaptive phenotypic traits of the annual plant *Arabidopsis thaliana* in ecologically realistic conditions. *Proc. Natl. Acad. Sci. U.S.A.* **113**: 3687-3692 (2016).
15. Li, H. *et al.* The sequence alignment/map format and SAMtools. *Bioinformatics* **25**, 2078-2079 (2009).
16. Koboldt, D.C. *et al.* VarScan 2: somatic mutation and copy number alteration discovery in cancer by exome sequencing. *Genome Res.* **22**, 568-576 (2012).
17. Roux, F. & Bergelson, J. The genetics underlying natural variation in the biotic interactions of *Arabidopsis thaliana*: the challenges of linking evolutionary genetics and community ecology. *Curr. Top. Dev. Biol.* **119**, 111-156 (2016).

18. Vailleau, F. *et al.* A R2R3-MYB gene, *AtMYB30*, acts as a positive regulator of the hypersensitive cell death program in plants in response to pathogen attack. *Proc. Natl. Acad. Sci. U.S.A.* **99**, 10179-10184 (2002).
19. Huard-Chauveau, C. *et al.* An atypical kinase under balancing selection confers broad-spectrum disease resistance in Arabidopsis. *PLoS Genet.* **9**, e1003766 (2013).
20. Atwell, S. *et al.* Genome-wide association study of 107 phenotypes in a common set of *Arabidopsis thaliana* inbred lines. *Nature* **465**, 627-631 (2010).
21. Kang, H.M. *et al.* Variance component model to account for sample structure in genome-wide association studies. *Nat. Genet.* **42**, 348-354 (2010).
22. Li, P. *et al.* Multiple *FLC* haplotypes defined by independent *cis*-regulatory variation underpin life history diversity in *Arabidopsis thaliana*. *Genes Dev.* **28,** 1635-1640 (2014).

Figure S1 | General picture of the TOU-A population. (**a**) Photograph showing the habitat type. The population is located under a 350m electric fence separating two permanent meadows. (**b**) Position of plants for which seeds have been collected in 2002, 2007 and 2010. (**c**) Position of soil samples collected in 2010. The letters A, B and C indicate the three edaphic areas (i.e. soil types) in which the *in situ* experiment has been performed (see **Supplementary Fig. 3**). (**d**) Tillage of the 10-cm upper soil layer in late August 2012 and protection from cattle by electric fences. (**e**) Soil cover with green plastic for weed control in late September 2012. (**f**) Observed natural germination flushes in late September 2012.

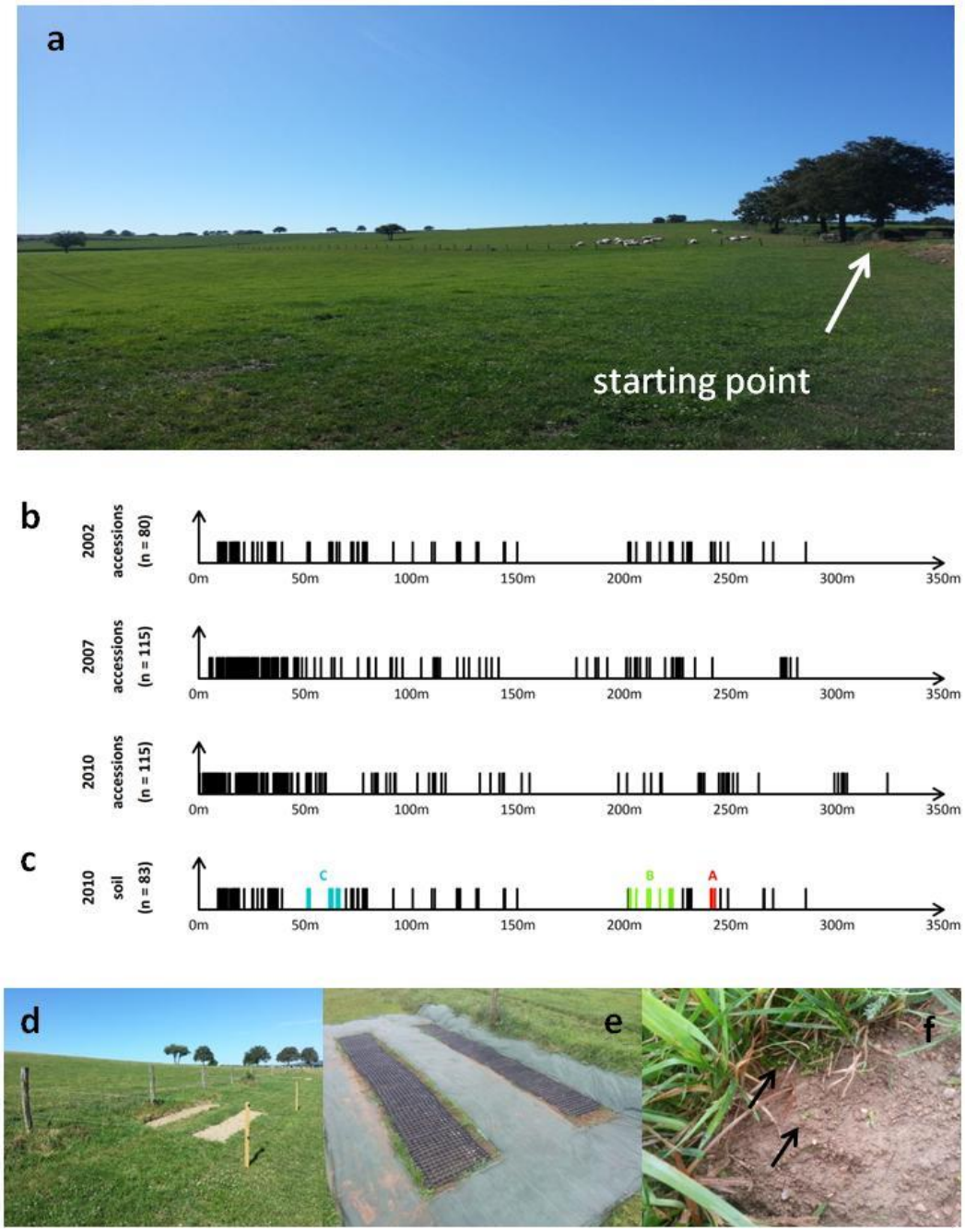

Figure S2 | Climate change since 1970 in the locality of the TOU-A population. Blue dots indicate the three sampling years (2002, 2007 and 2010). The green dot indicates the year of the *in situ* experiment. Red lines correspond to the mean of the last five consecutive years. A significant change over time was detected for the mean annual temperature (Spearman's *rho* = 0.63, $P = 5.5 \times 10^{-6}$), the mean warmest month temperature (Spearman's *rho* = 0.35, $P = 0.019$) and the sum of degree-days above 5°C (Spearman's *rho* = 0.69, $P = 7.1 \times 10^{-7}$), but not for the mean coldest month temperature (Spearman's *rho* = 0.-0.026, $P = 0.865$), the mean annual precipitation (Spearman's *rho* = 0.025, $P = 0.869$) and the sum of degree-days below 0°C (Spearman's *rho* = -0.090, $P = 0.560$).

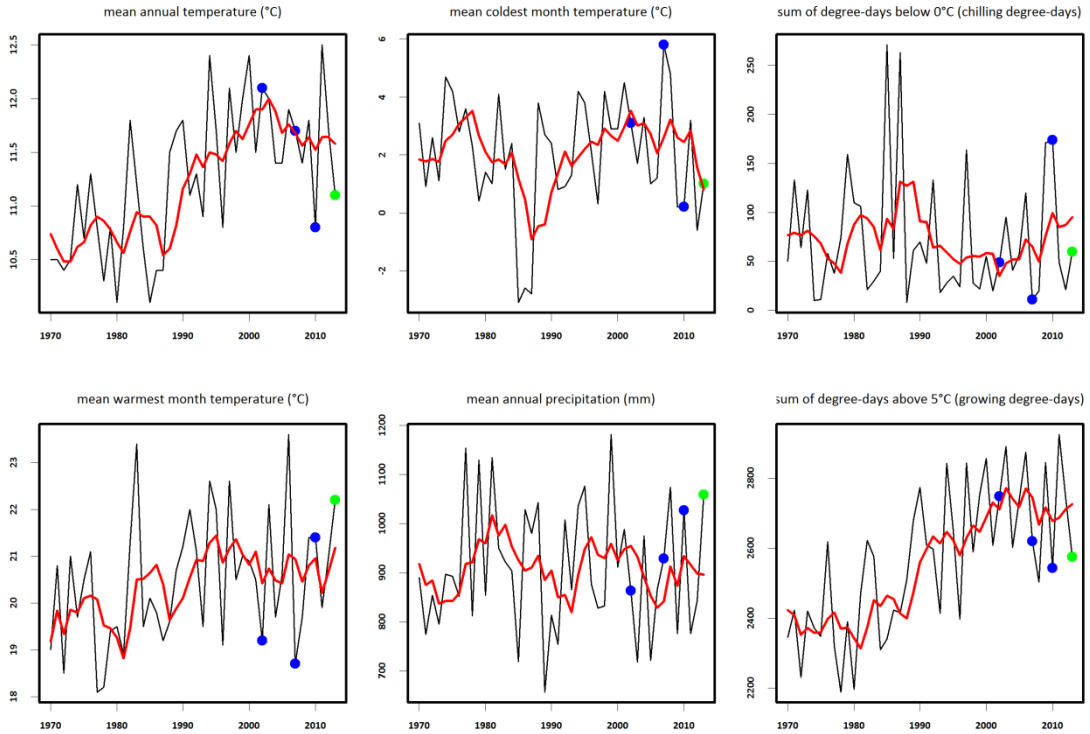

Figure S3 | Edaphic variation in the TOU-A population. (**a**) Factor loading plot resulting from principal components analysis. Factor 1 and factor 2 explained 31.54% and 24.22% of total soil variance. Maximum water holding capacity (WHC), content of total nitrogen (N), organic carbon / total nitrogen ratio (C.N), concentrations of P_2O_5, K, Mg, Mn, Al and Na. (**b**) Distribution of eigenvalues against the ranked component number. (**c**) Position of the 83 soil samples in the 'Factor1 – Factor 2' edaphic space. Red, green and blue dots correspond to the soil samples located in three soil areas 'soil A', 'soil B' and 'soil C', respectively.

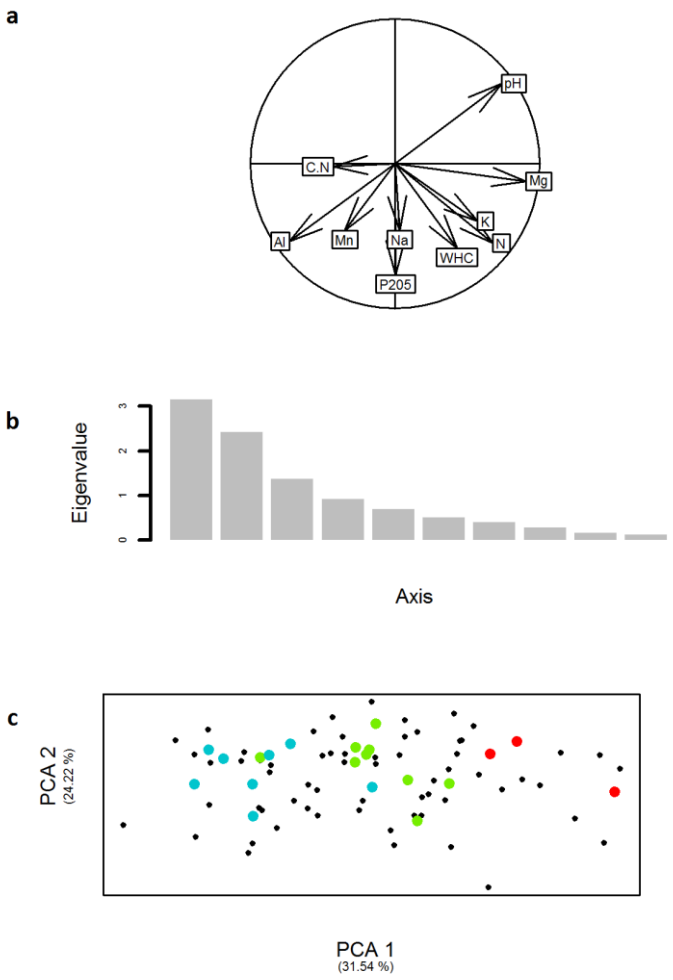

Figure S4 | Distribution of across-micro-habitat genetic correlations calculated for each phenotypic trait. For each of the 29 traits, we calculated the pairwise genetic correlations among the micro-habitats (Pearson correlation coefficient), by considering only the micro-habitats in which the trait displayed significant genetic variance (i.e. heritable eco-phenotypes, Figure 1).

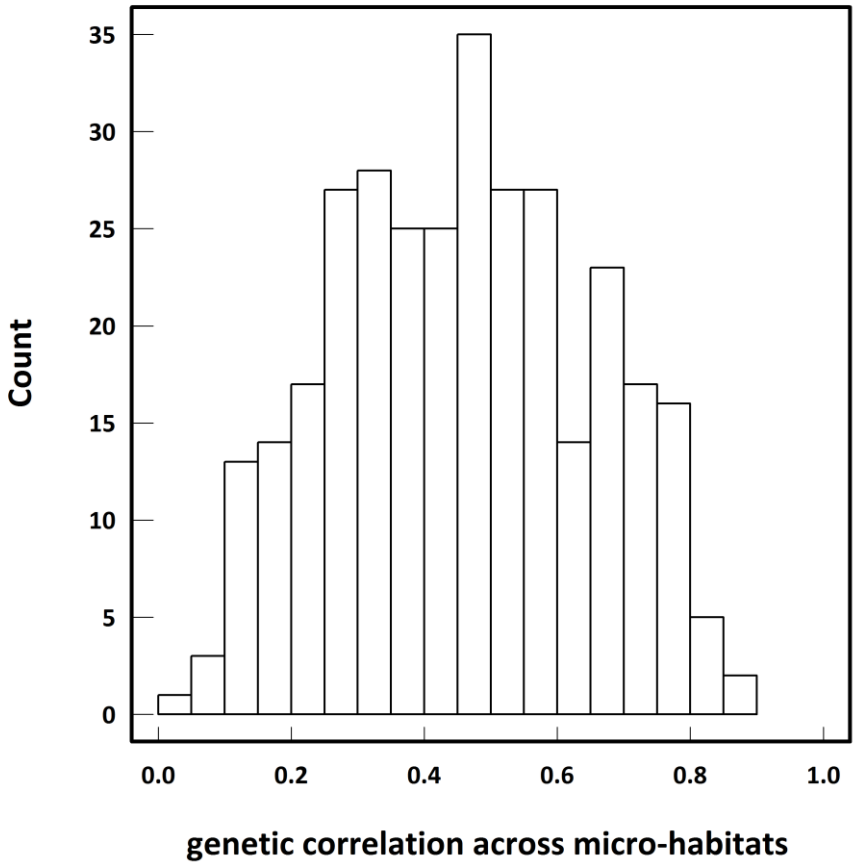

Figure S5 | Illustration of the genotype-by-environment interactions across the six *in situ* 'soil x competition' micro-habitats. (**a**) Genetic variation for reaction norms of bolting time. (**b**) Genetic variation for reaction norms of seed production on the main stem. Solid red lines: reaction norms of the 80 accessions collected in 2002, dashed blue lines: reaction norms of the 115 accessions collected in 2010.

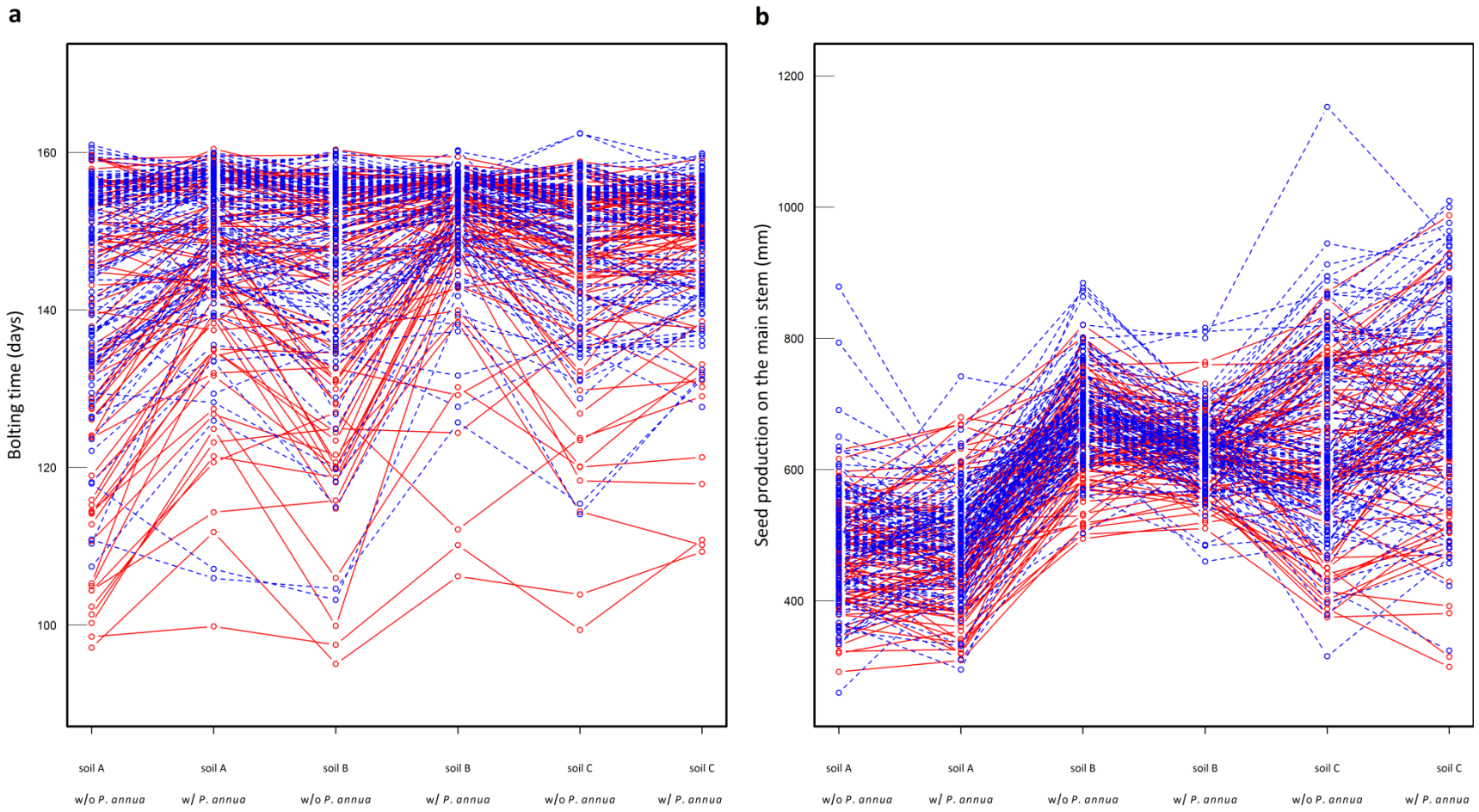

Figure S6 | Distribution of the size of LD blocks in the TOU-A population.

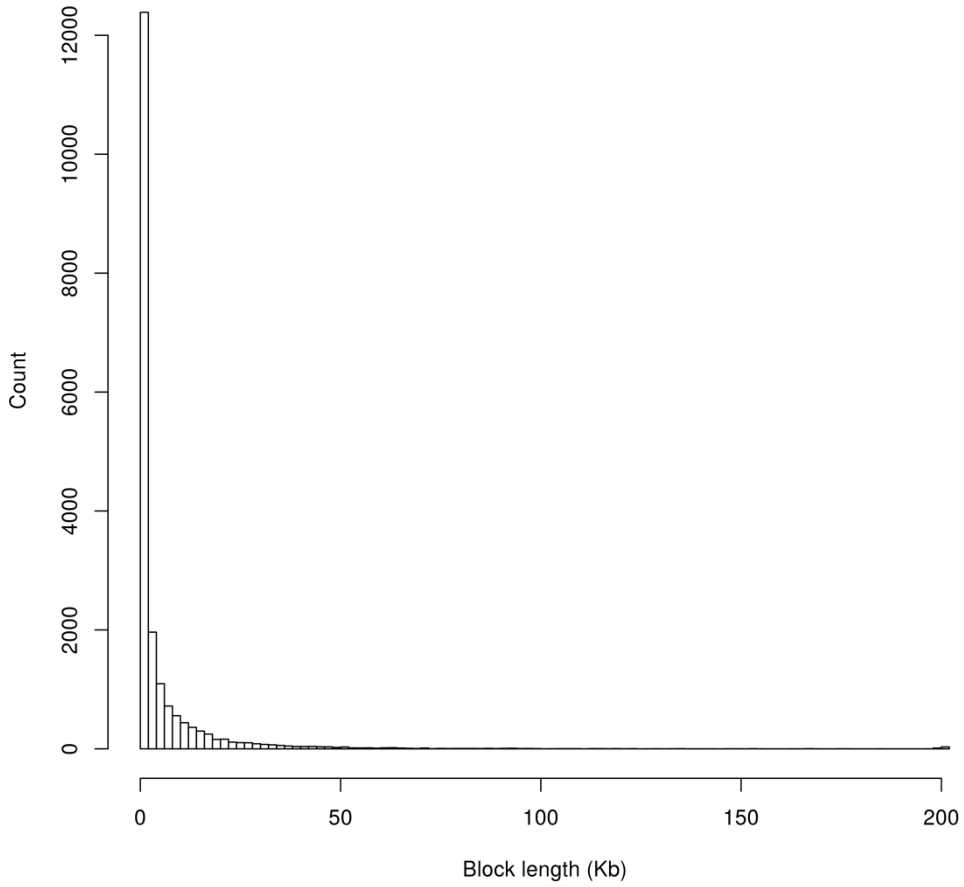

Figure S7 | GWA analysis of hypersensitive response to the bacterial elicitors *AvrRpm1* (a) and *AvrRpt2* (b) and quantitative resistance to *Xanthomonas campestris* pv. *campestris* strain *Xcc568* (c). The top SNPs are located 15bp from *RESISTANCE TO PSEUSOMONAS SYRINGAE PV MACULICOLA* (*RPM1*), within *RESISTANT TO PSEUDOMONAS SYRINGAE 2* (*RPS2*) and within *RESISTANCE RELATED KINASE 1* (*RKS1*). The *x*-axis indicates the physical position along the chromosome. The *y*-axis indicates the -log^{10} *p*-values of phenotype-SNP associations using the EMMAX method. MARF > 7%.

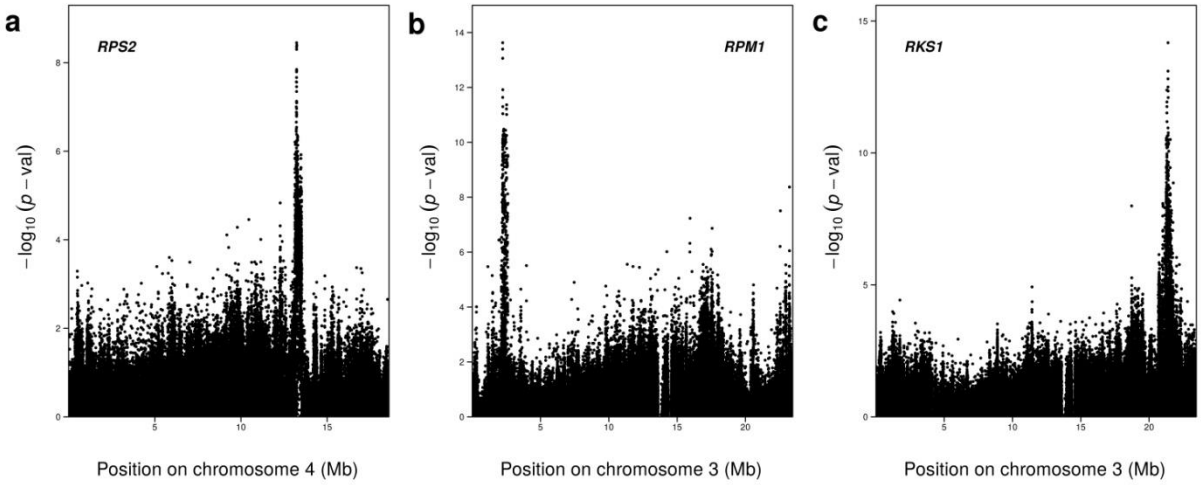

Figure S8 | Enrichment ratios in flowering time candidate genes for the six *in situ* 'soil x competition' micro-habitats (i.e. three soils A, B and C x absence or presence of *P. annua*), as a function of the number of top SNPs chosen in the GWA mapping results for bolting time using the EMMAX method. The corresponding 95% confidence intervals from the null distributions are represented by the green area.

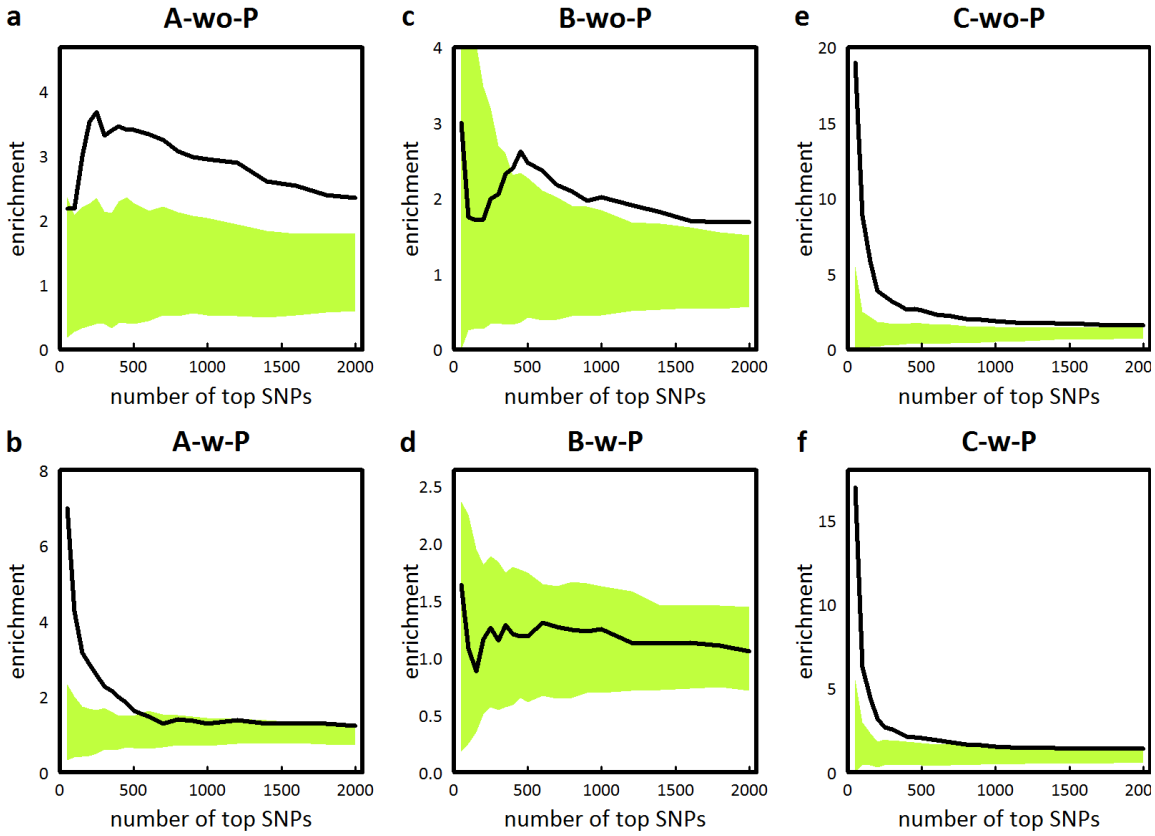

Figure S9 | Identification of genomic regions associated with the 144 heritable eco-phenotypes in the TOU-A population. The *x*-axis indicates the physical position along the chromosome. The *y*-axis indicates the -log^{10} *p*-values using the EMMAX method. MARF > 7%. On each Manhattan plot, the 100 and 200 top SNPs are highlighted in blue and red, respectively.

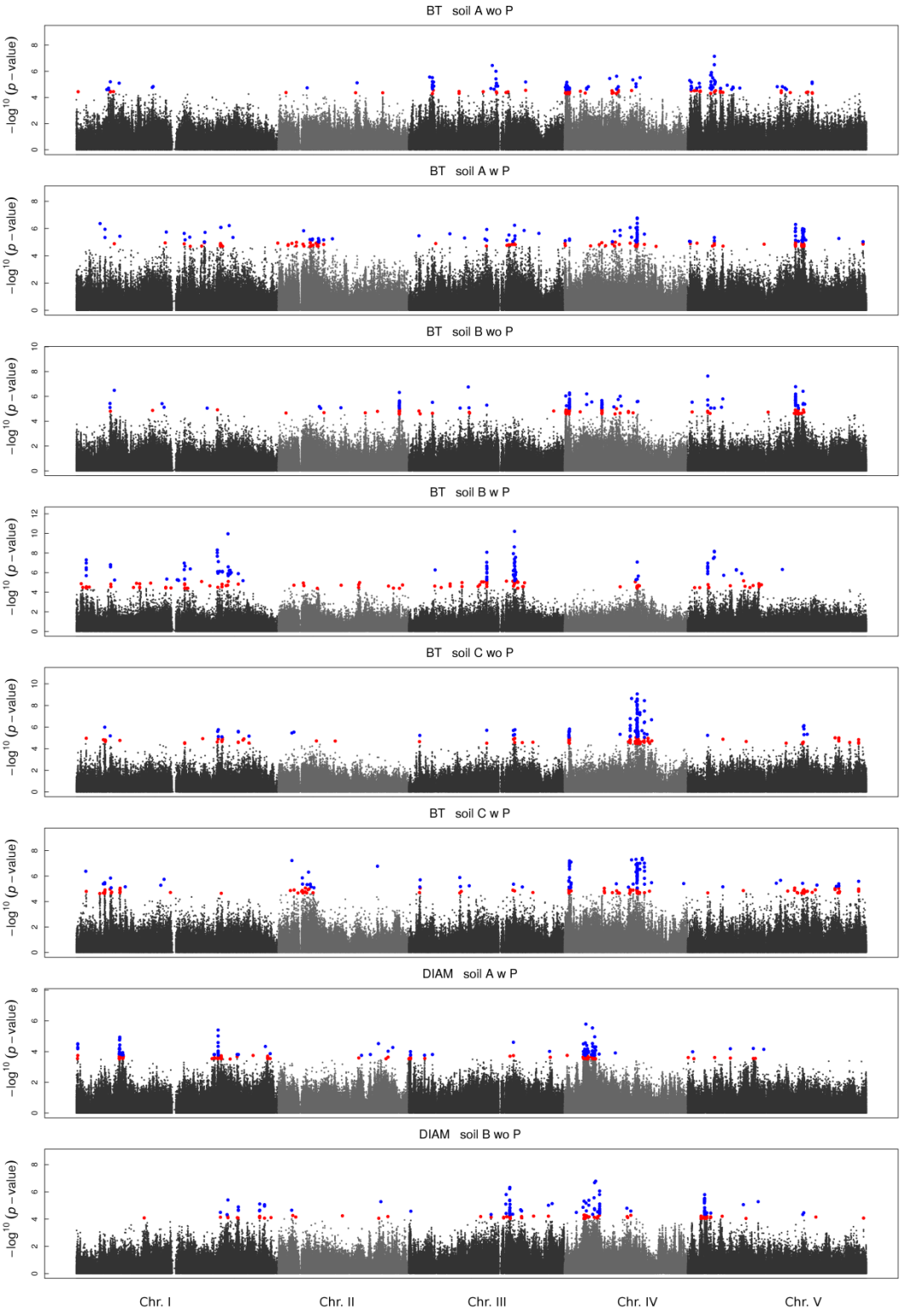

Figure S9 (continued)

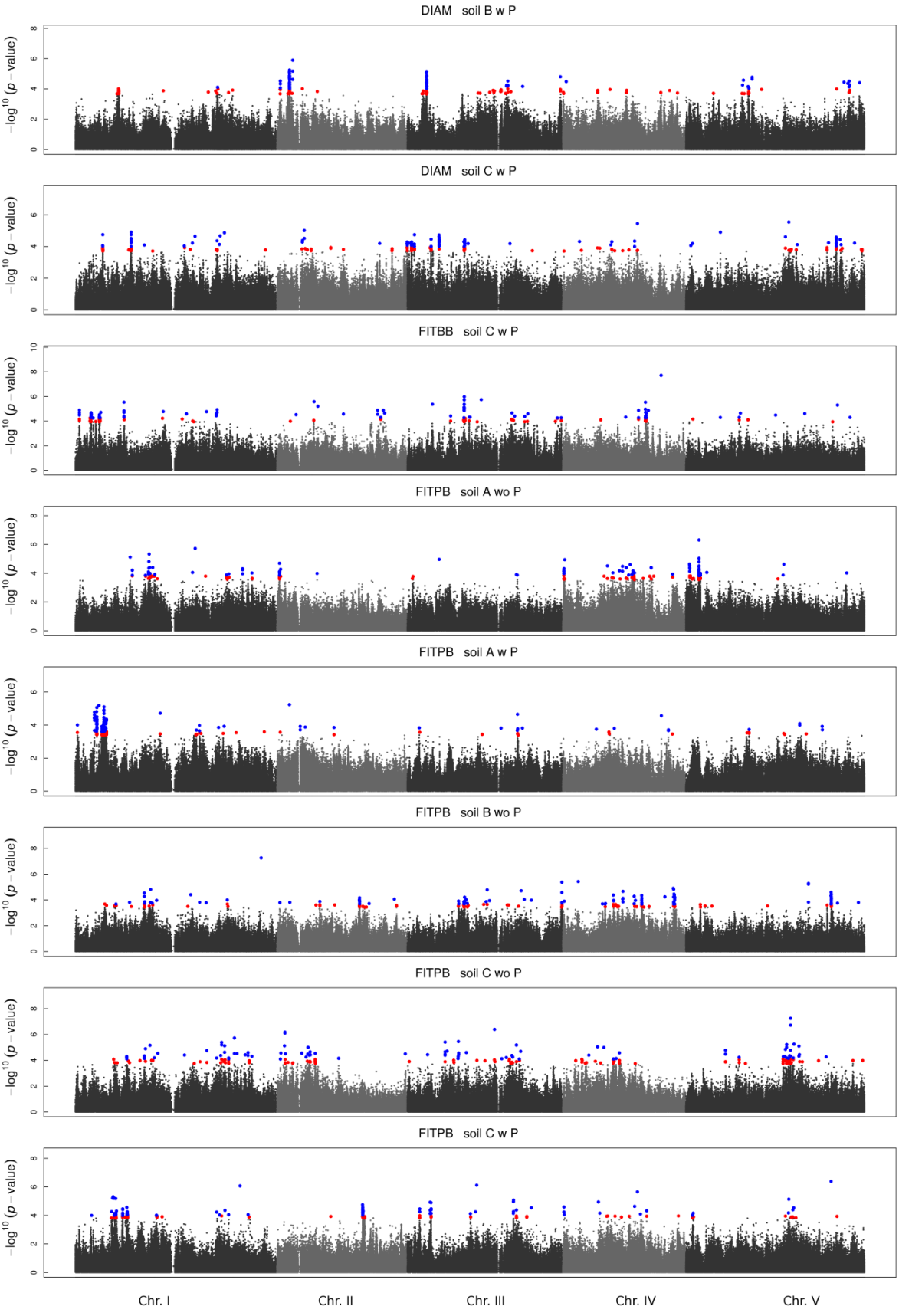

Figure S9 (continued)

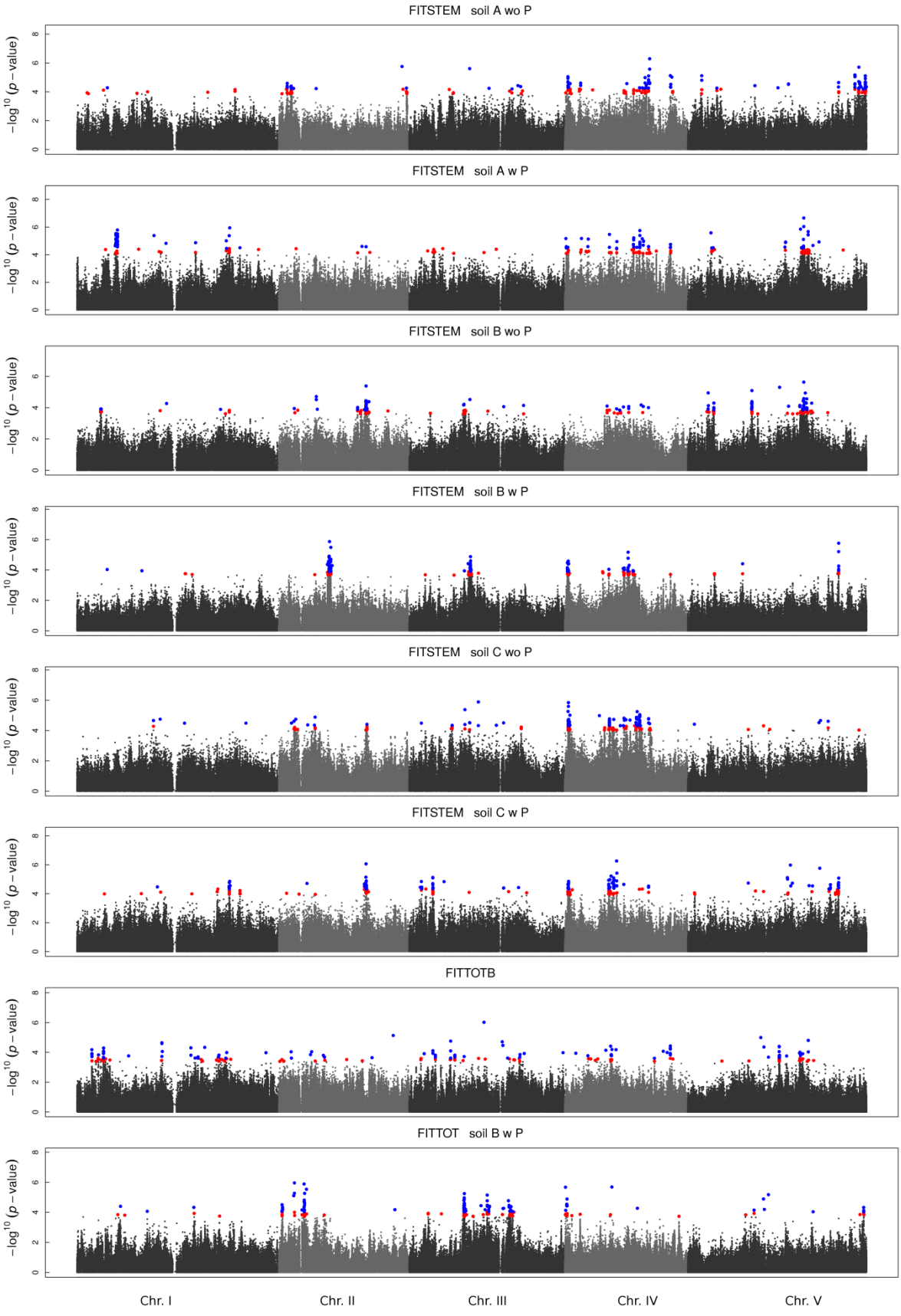

Figure S9 (continued)

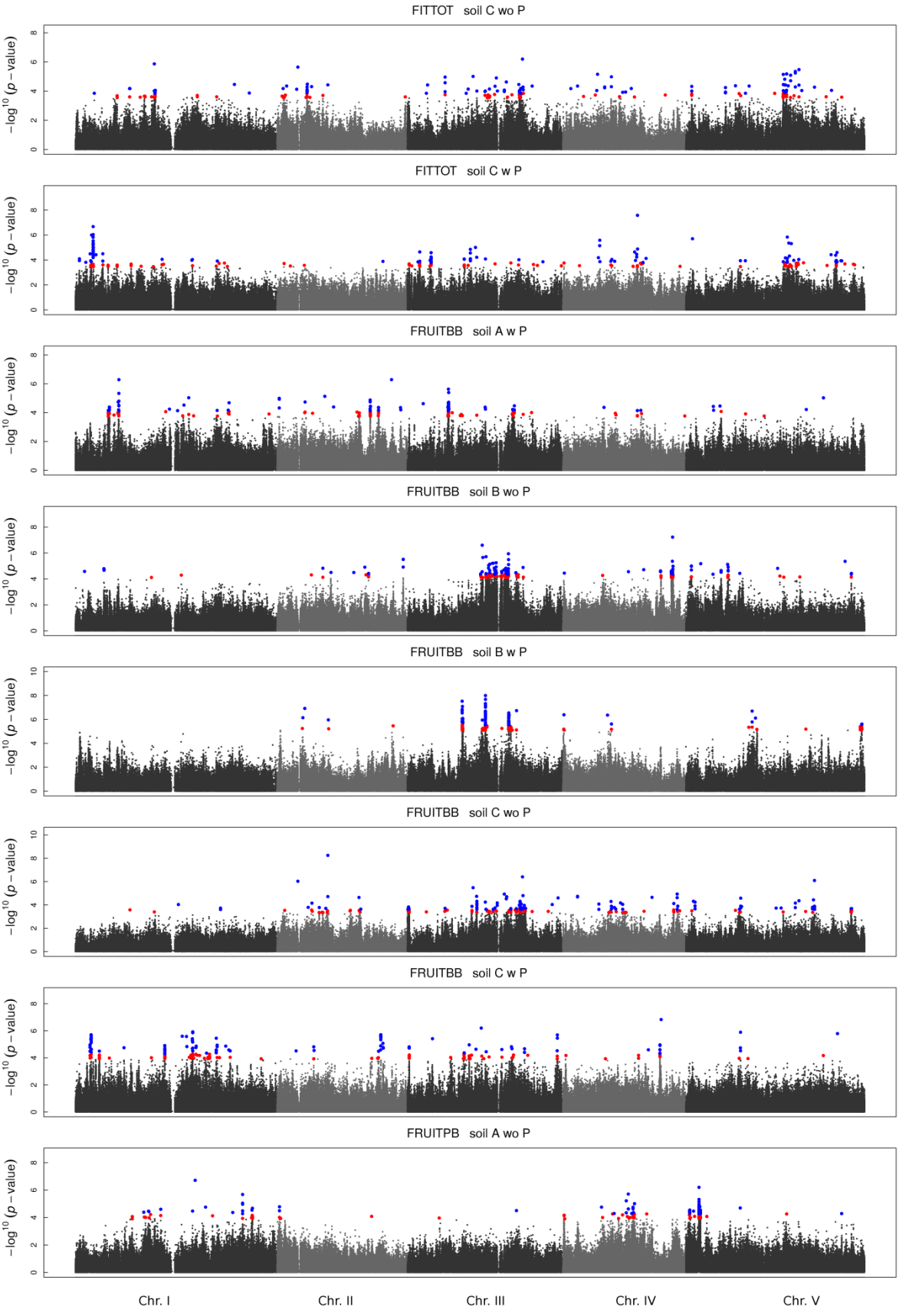

Figure S9 (continued)

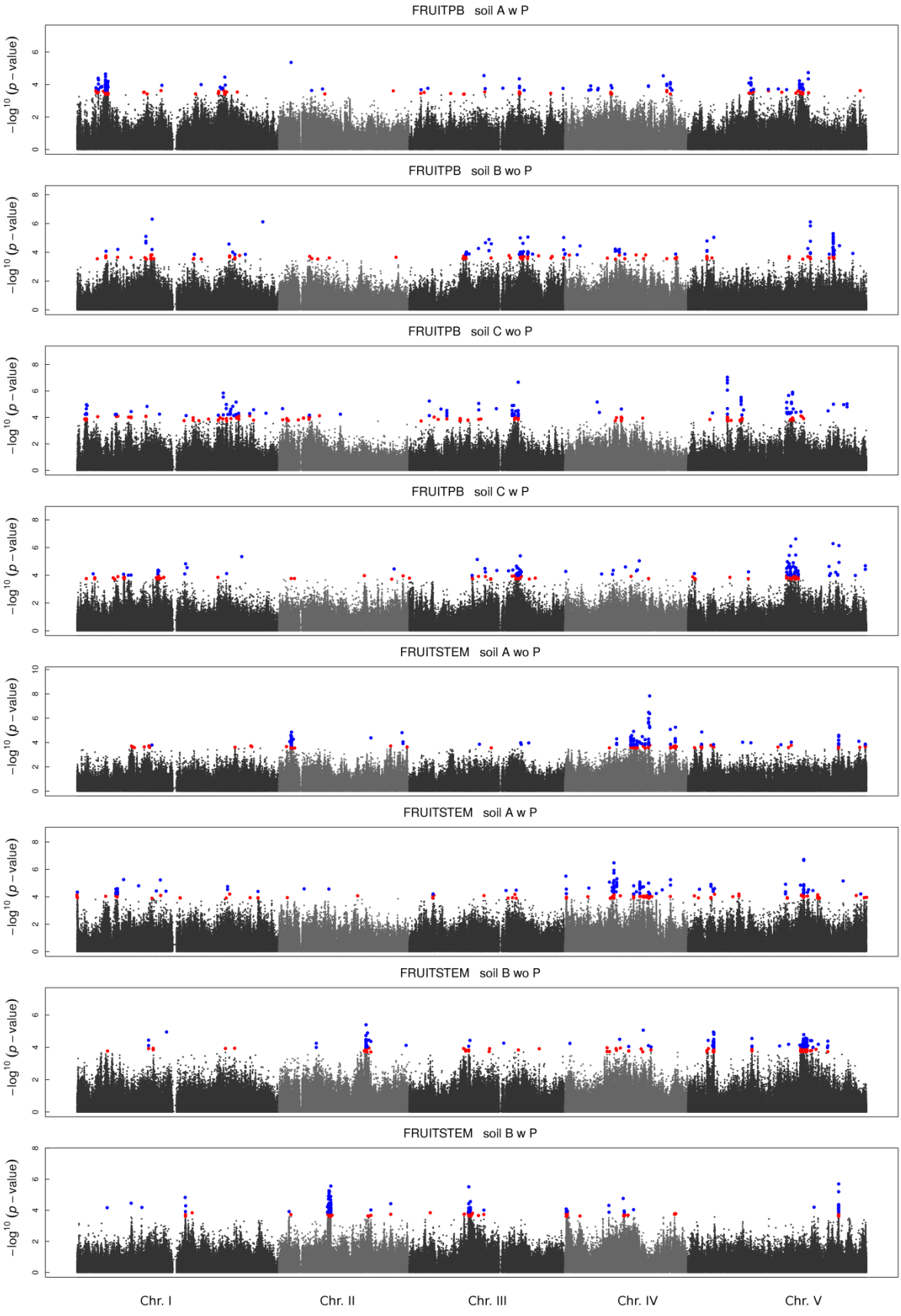

Figure S9 (continued)

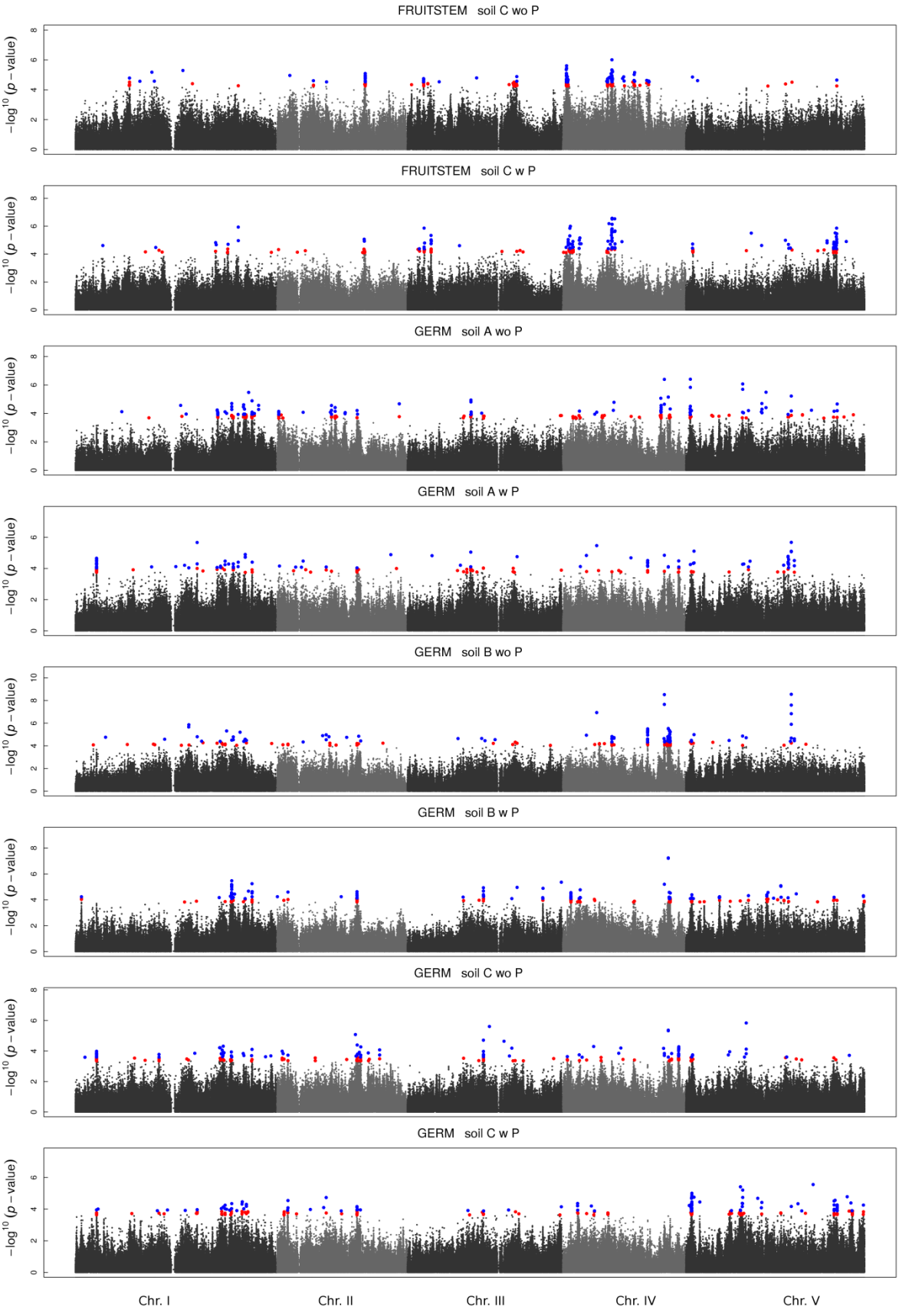

Figure S9 (continued)

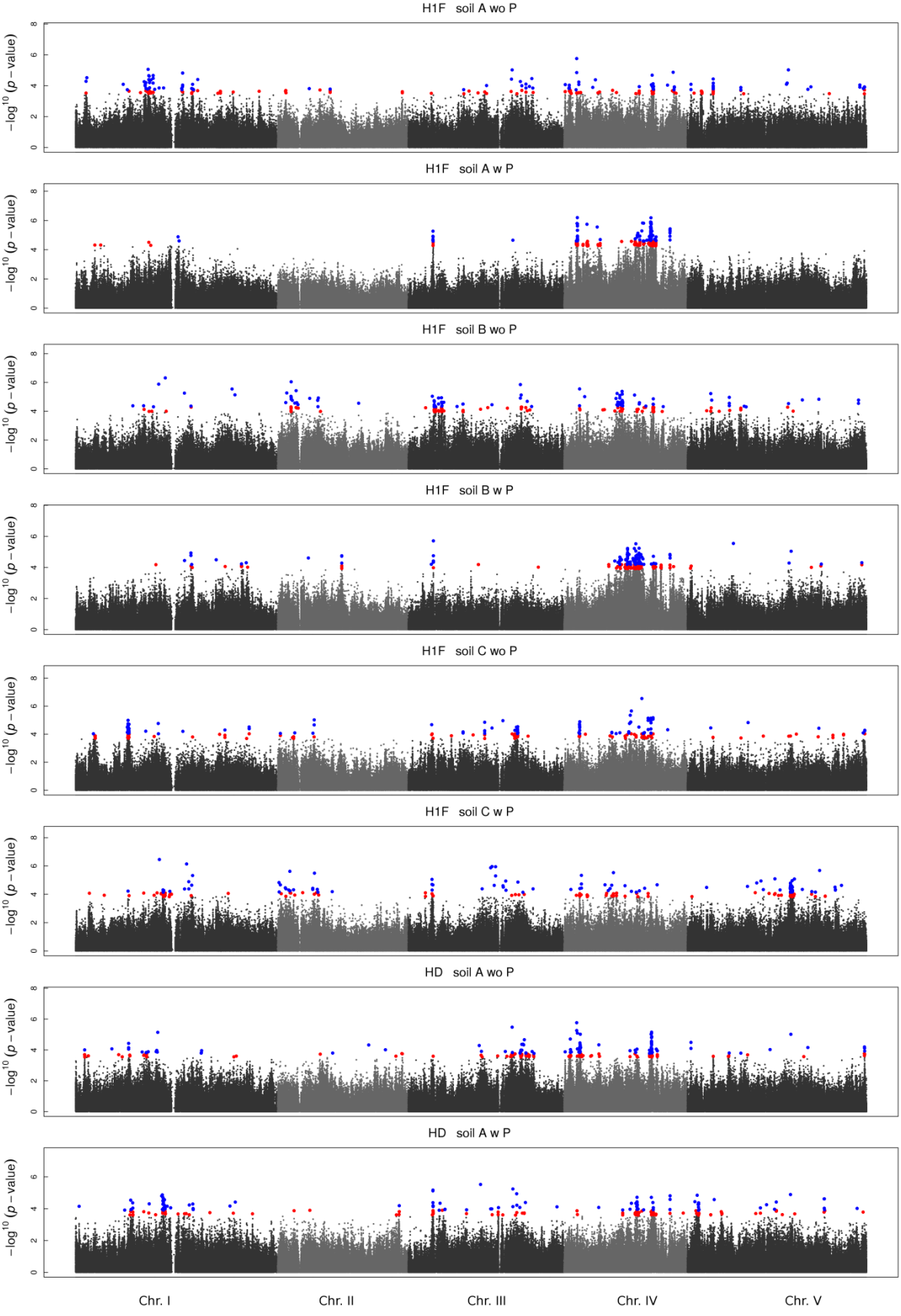

Figure S9 (continued)

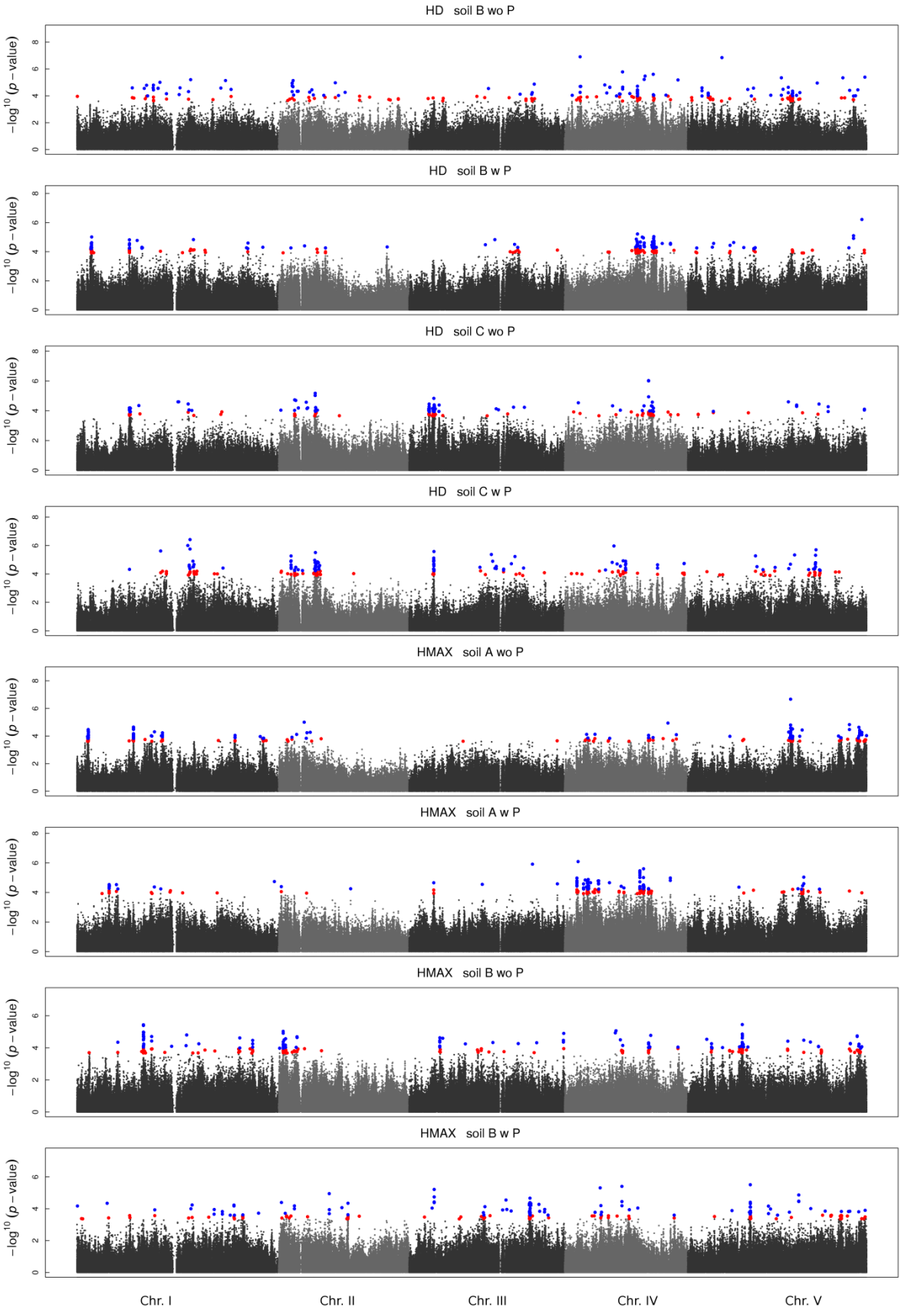

Figure S9 (continued)

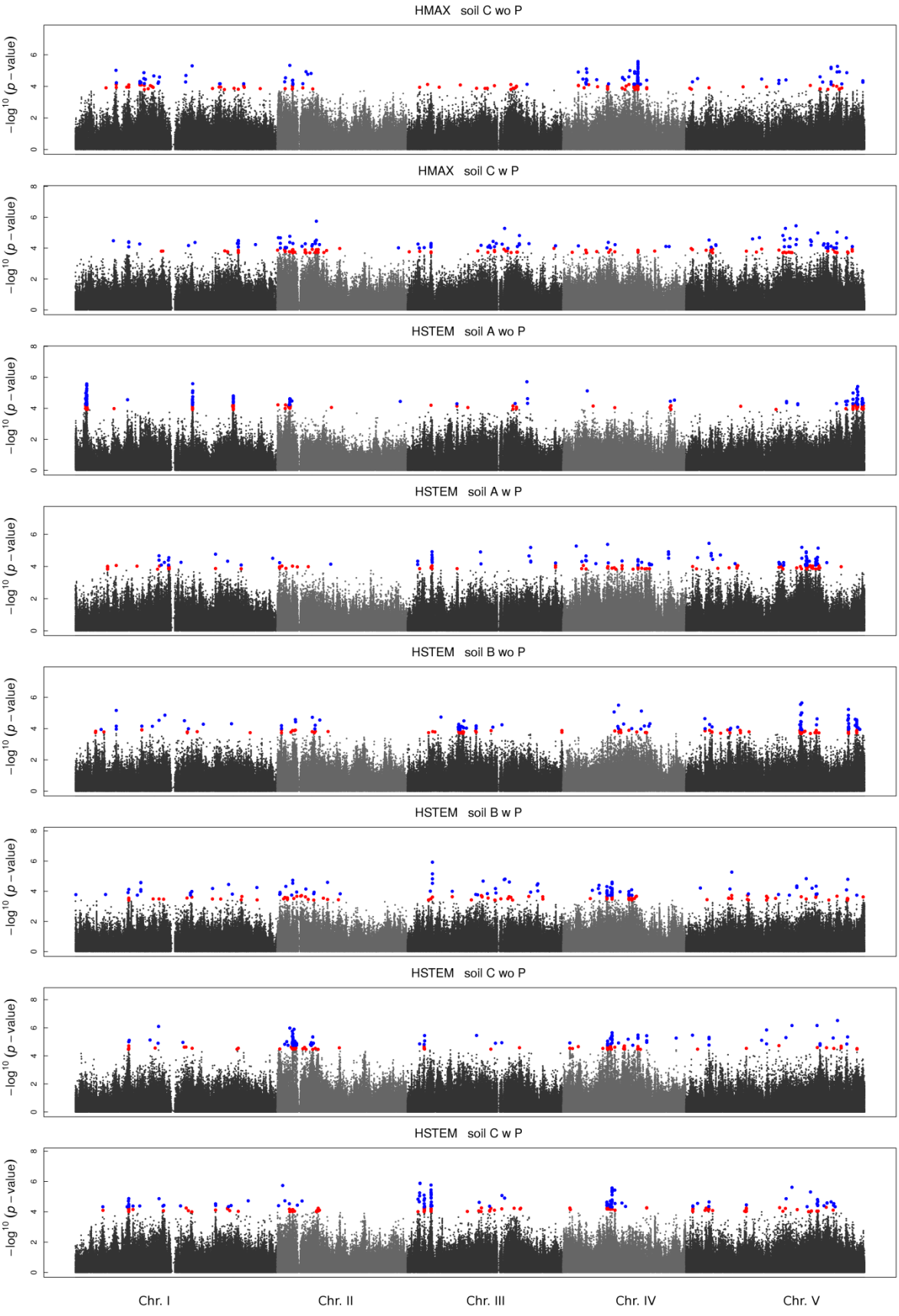

Figure S9 (continued)

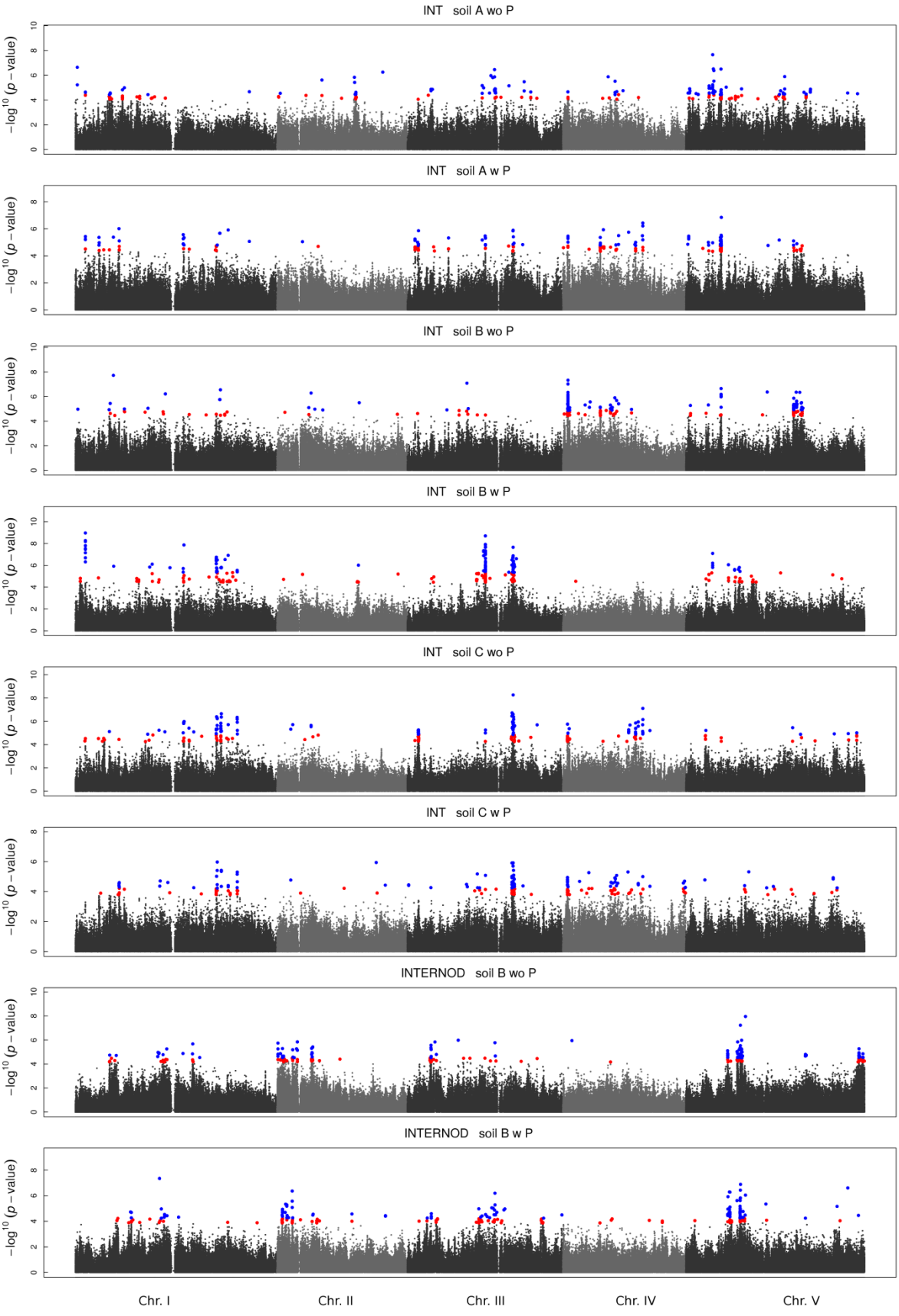

Figure S9 (continued)

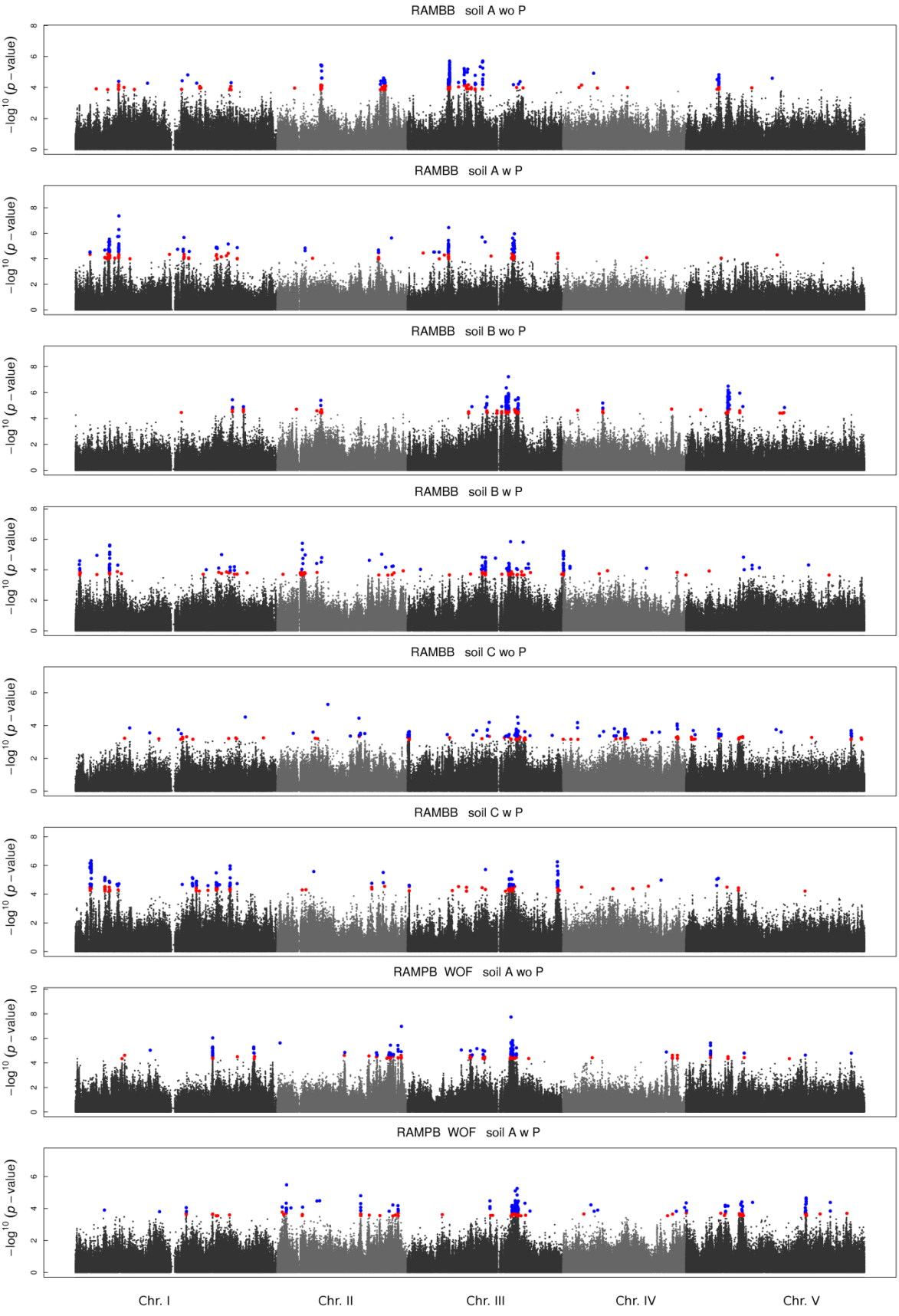

Figure S9 (continued)

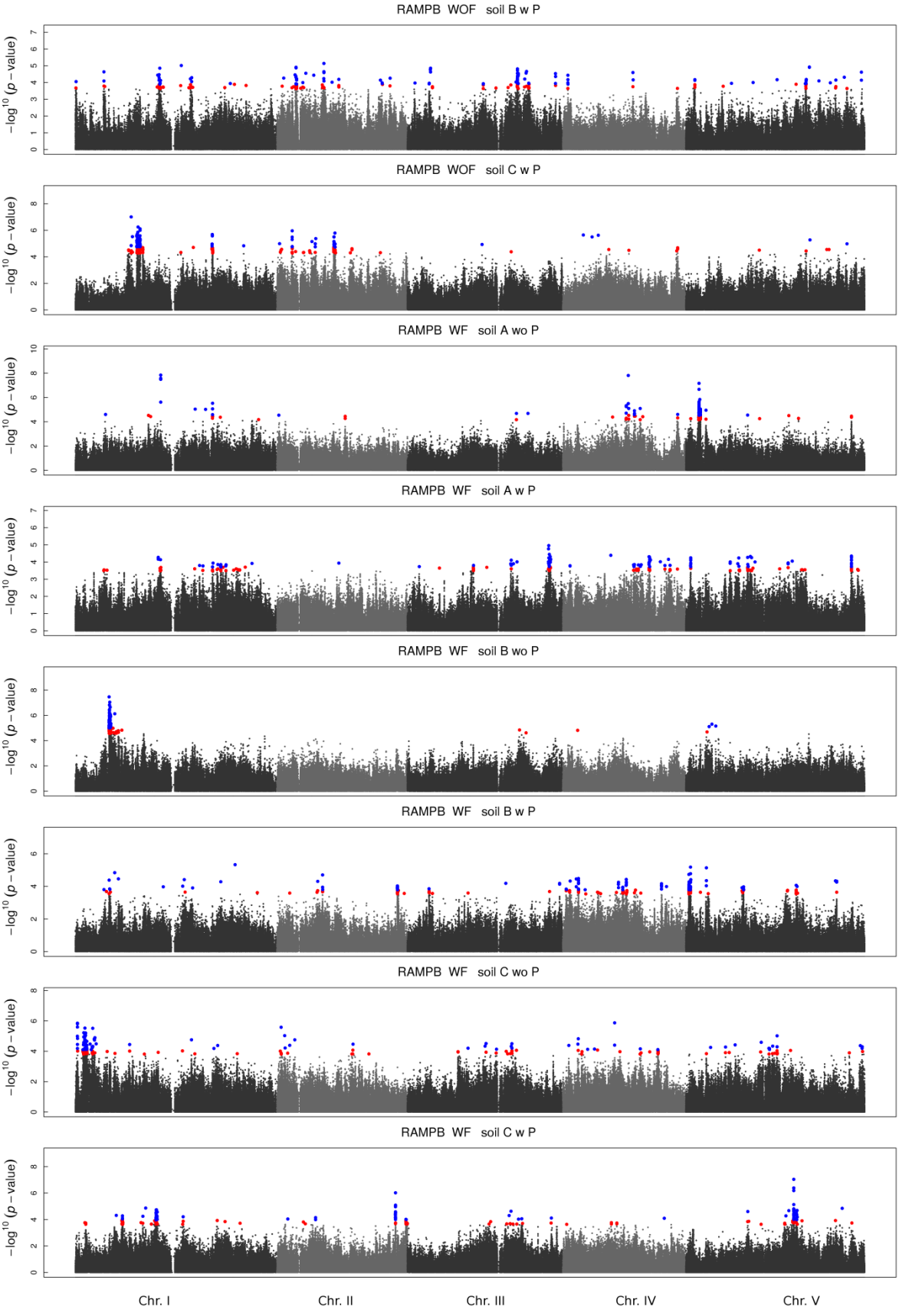

Figure S9 (continued)

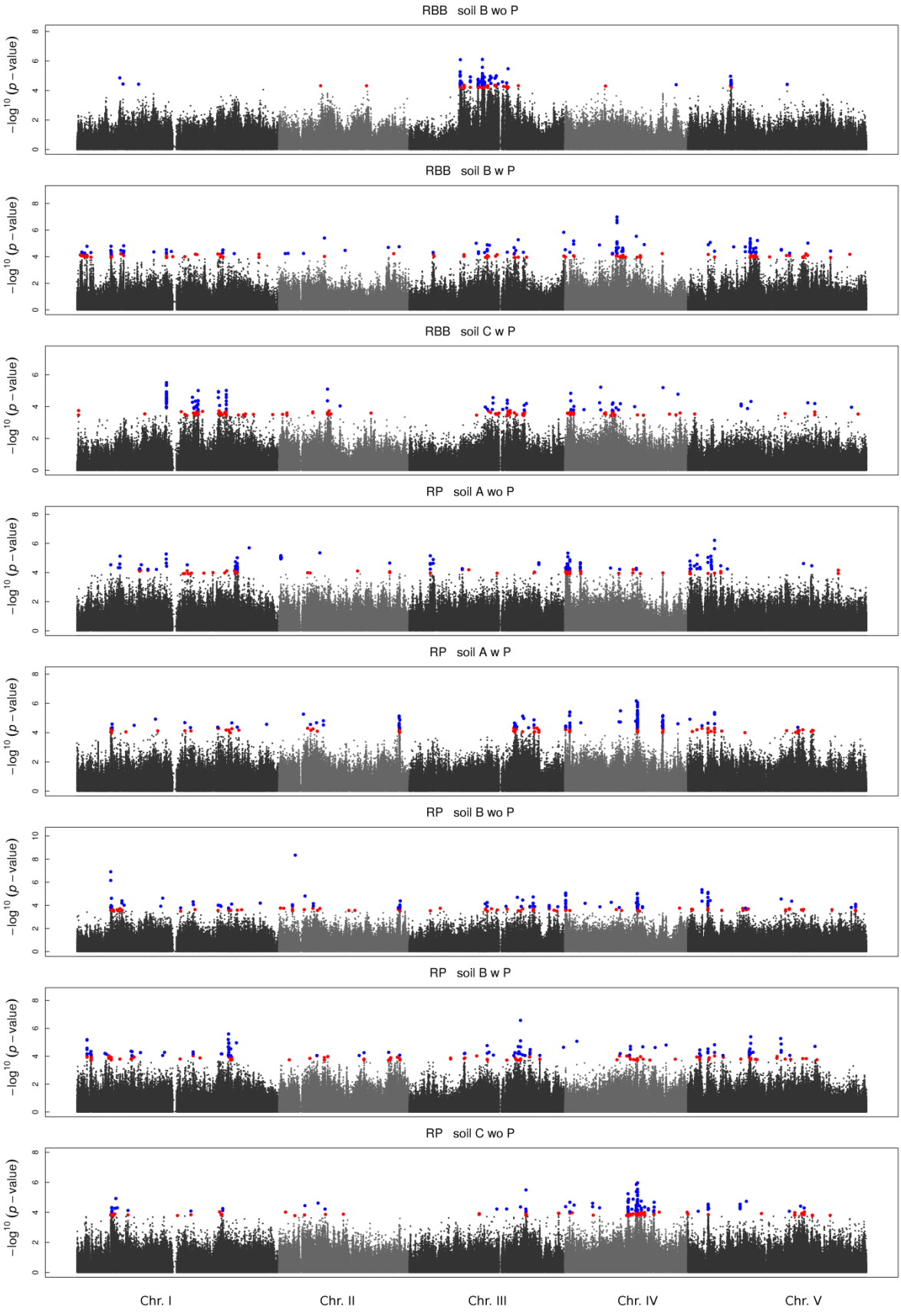

Figure S9 (continued)

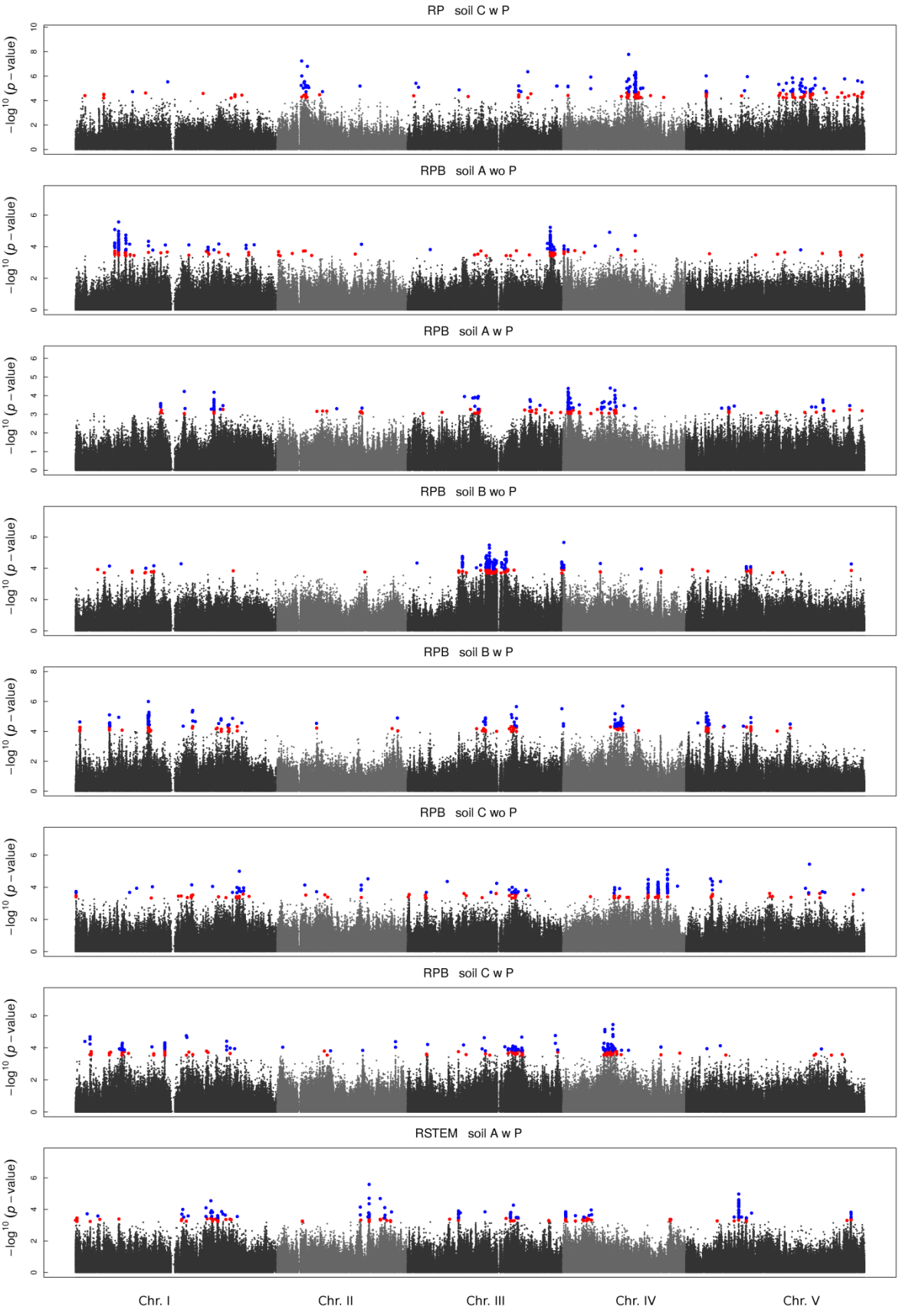

Figure S9 (continued)

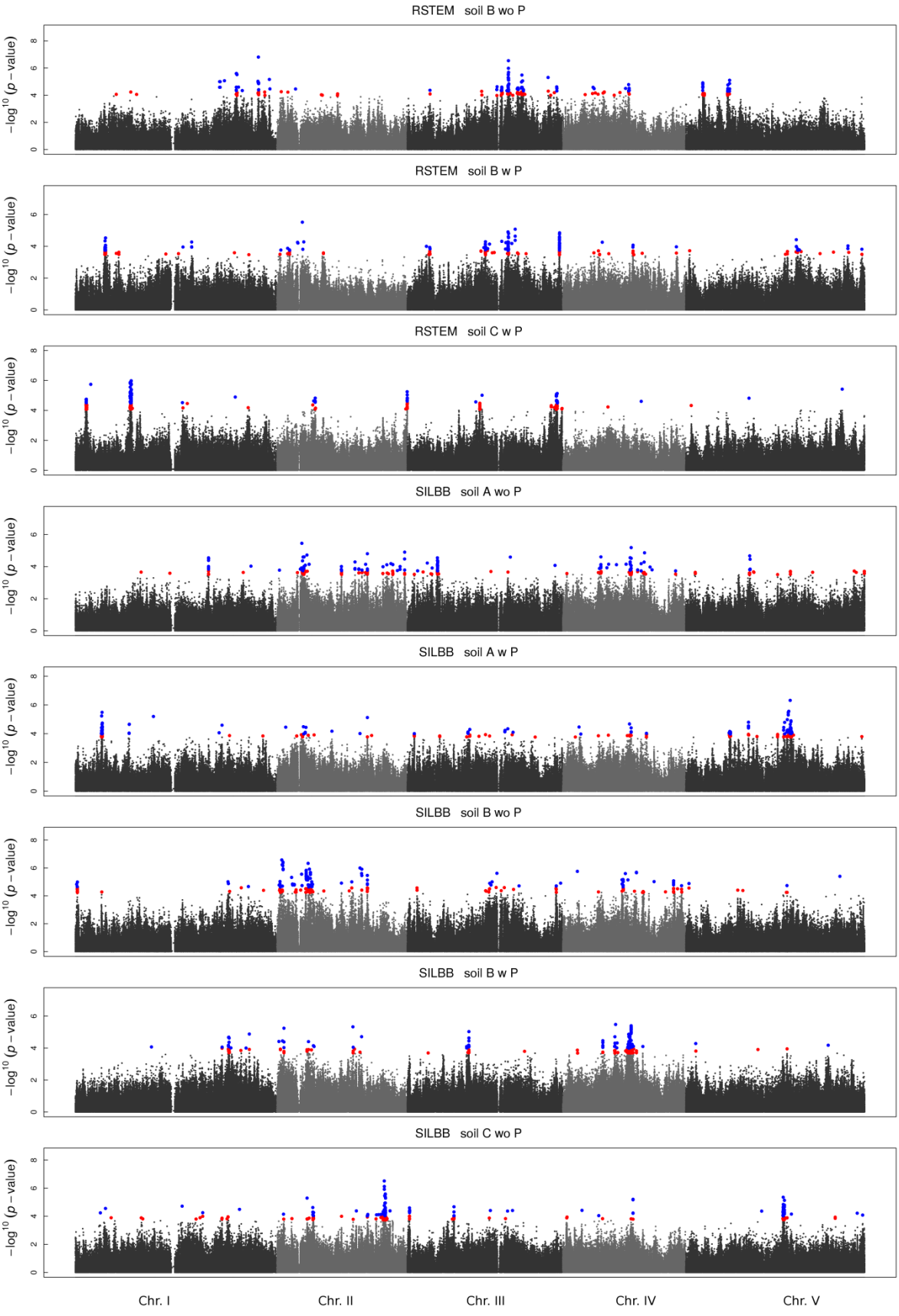

Figure S9 (continued)

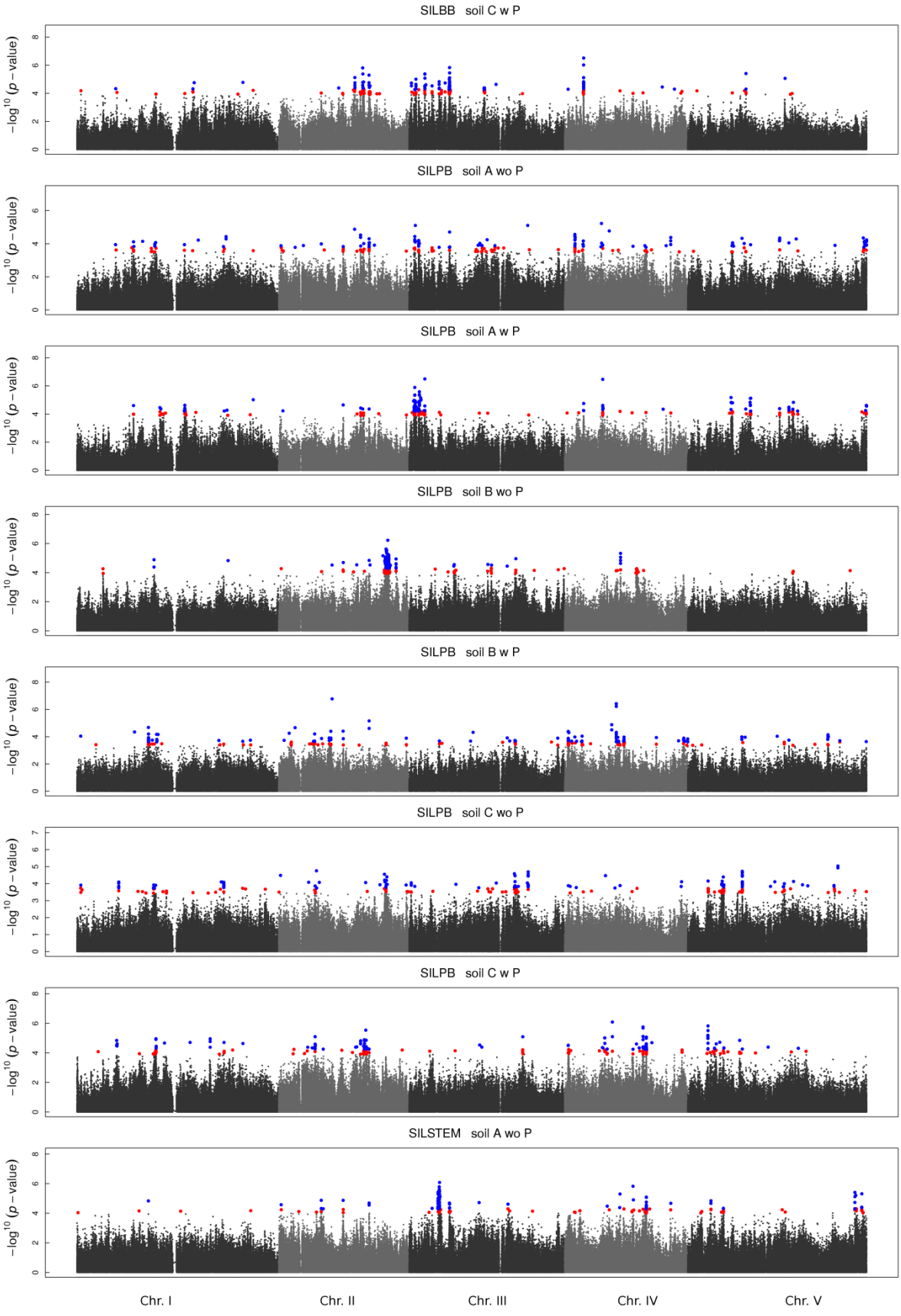

Figure S9 (continued)

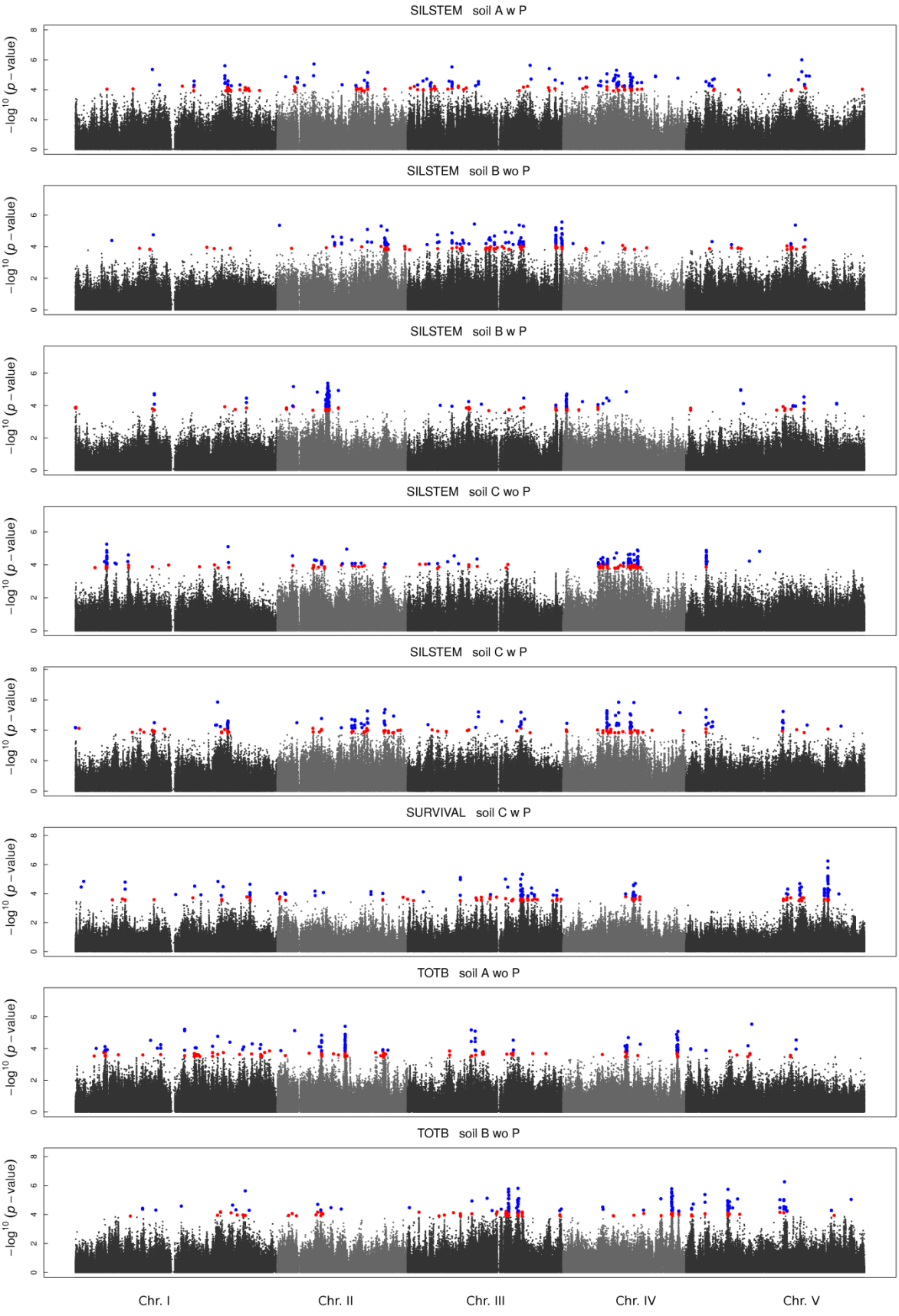

Figure S9 (continued)

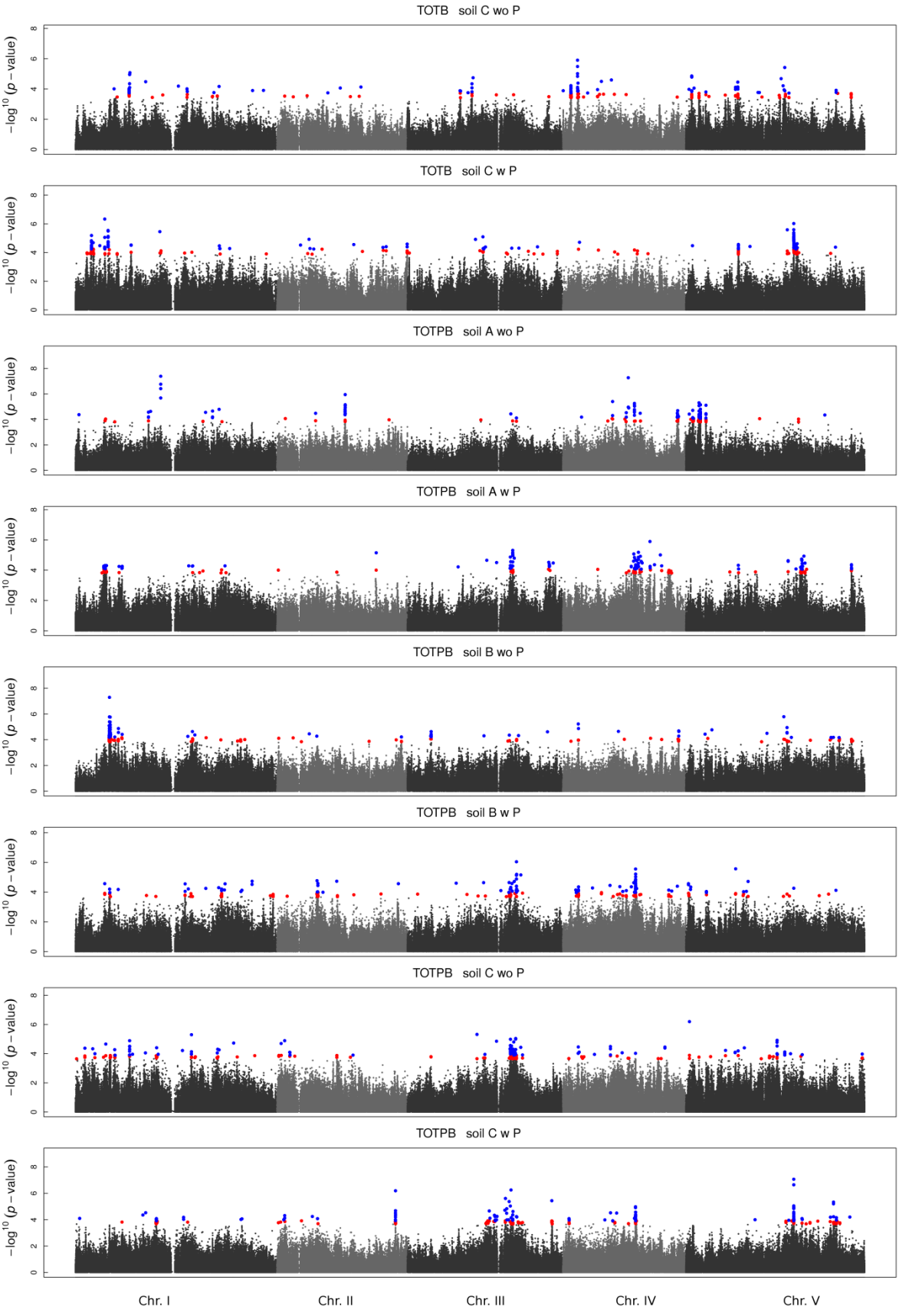

Figure S10 | Number of genes represented in the top 200 SNPs for each of the 144 heritable eco-phenotypes. Genes have been retrieved in a 1kb window size on each side of each top SNP.

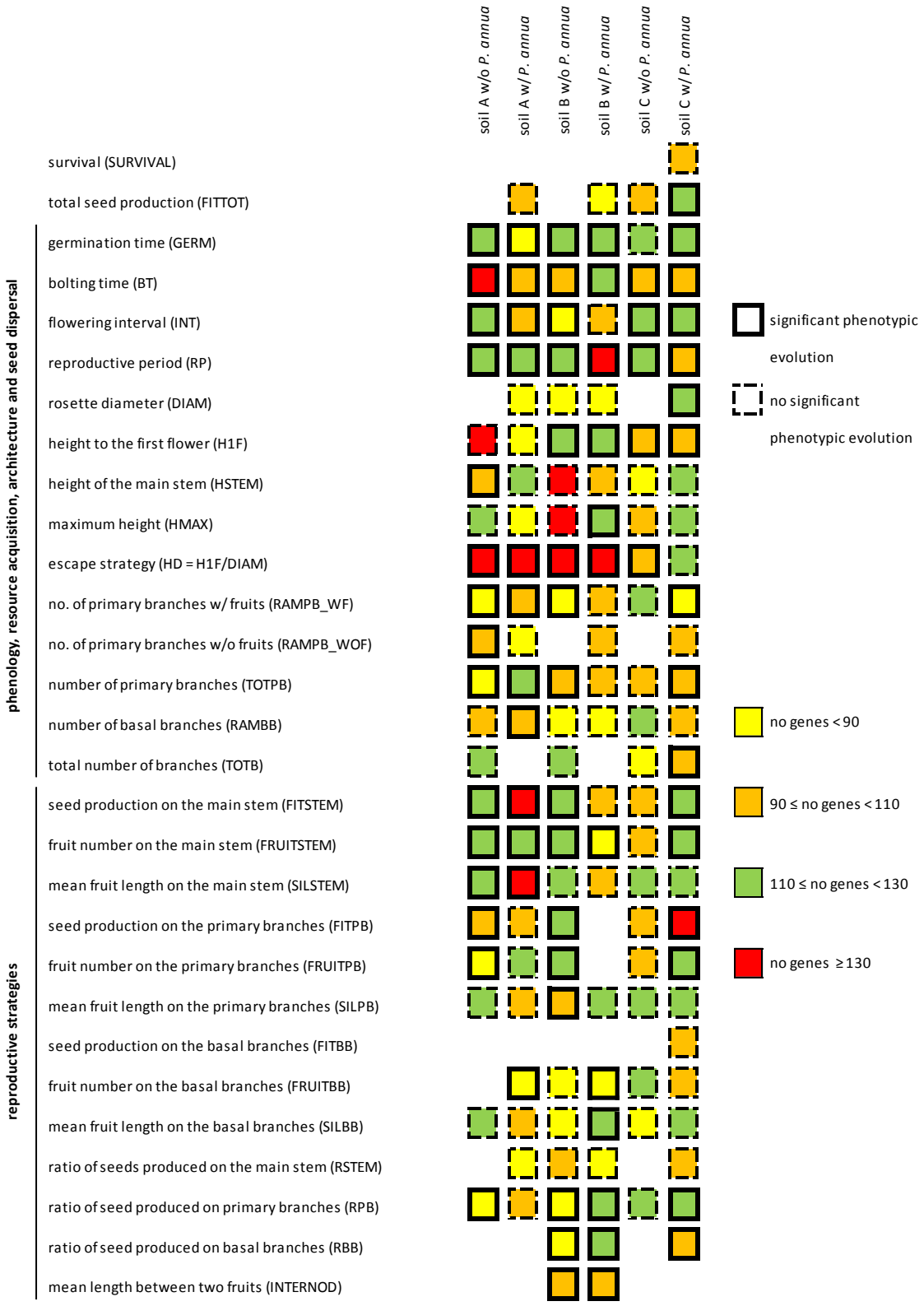

Figure S11 | Comparison of the standardized allelic effect *A* for bolting time among the six micro-habitats. N = 200 top SNPs for each micro-habitat. Different letters indicate significant differences between two micro-habitats at $P = 0.05$ (after Tukey's HSD test).

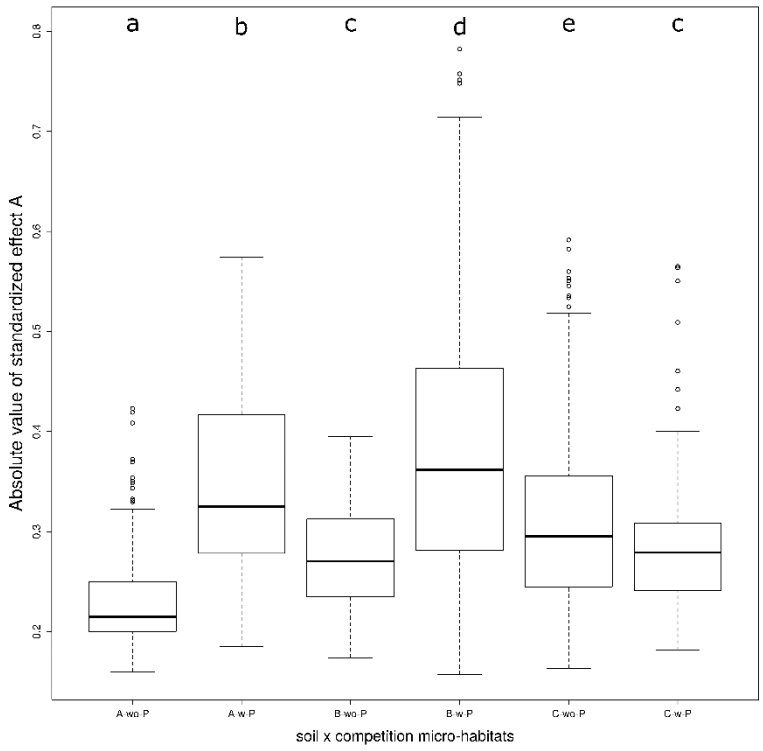

Figure S12 | Non proportional Venn diagram presenting the partitioning of top SNPs associated with the 144 heritable eco-phenotypes between the six *in situ* 'soil x competition' micro-habitats. (i.e. three soils A, B and C x absence or presence of *P. annua*). Numbers in brackets indicate the number of eco-phenotypes for each *in situ* 'soil x competition' micro-habitat.

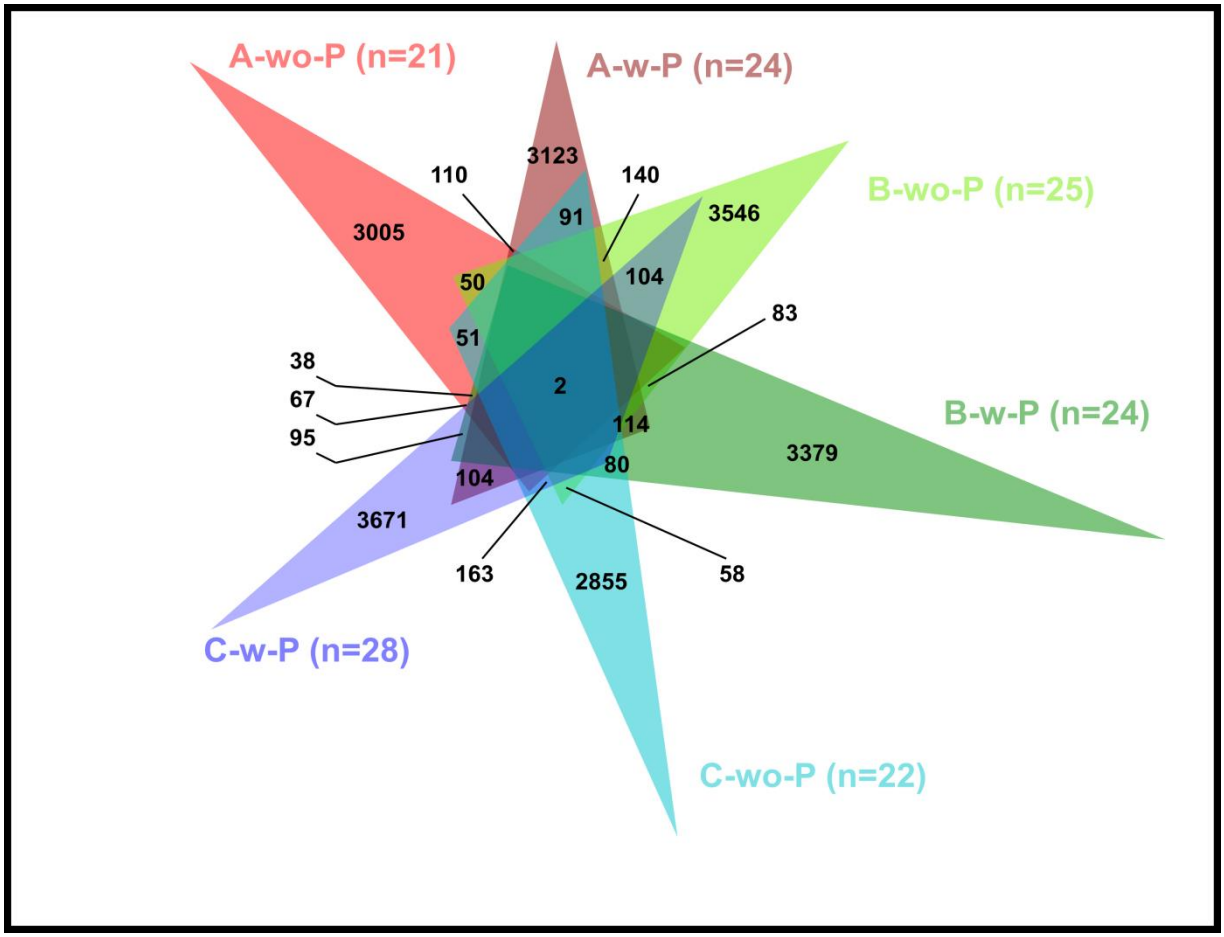

Figure S13A | Degree of pleiotropy and pleiotropic scaling in the TOU-A population when considering a threshold of 50, 100, 300 and 500 top SNPs. (**Top panels**) Frequency distribution of the effective number of eco-phenotypes affected by a SNP (N_{eff}, accounting for the correlations between eco-phenotypes) among the 21,268 unique top SNPs. (**Bottom panels**) Regression of total effect size T_M (total effect size by the Manhattan distance) on N_{eff}. The formula corresponds to the pleiotropic scaling relationship $\boldsymbol{T_M = c^* N_{eff}^{\,d}}$. A scaling component d exceeding 1 indicates that the mean per-trait effect size of a given top SNP increased with N_{eff}[8]. Solid red line: fitted relationship between T_M and N_{eff}, solid black line: linear dependence ($d = 1$).

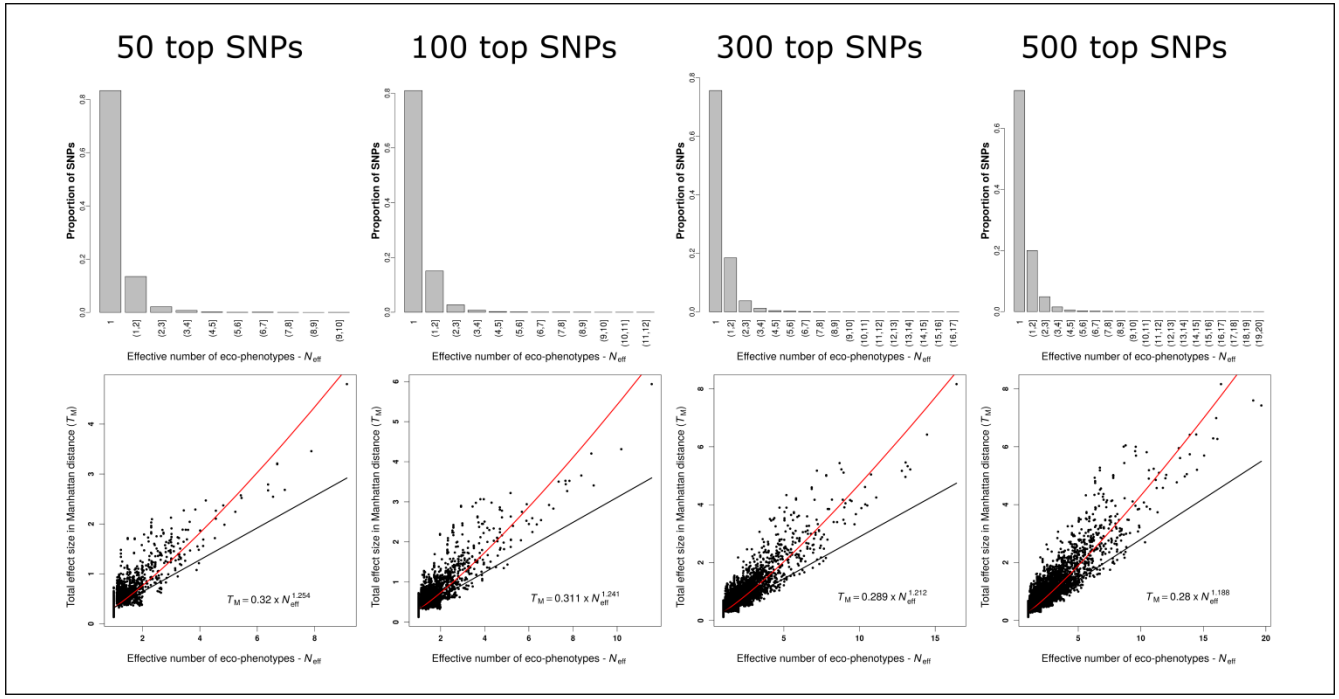

Figure S13B | Significance and strength of selection in the TOU-A population when considering a threshold of 50, 100, 300 and 500 top SNPs. (**Top panels**) Fold-increase in median $-\log_{10}$ (p-values) of neutrality tests based on temporal differentiation for SNPs that hit only evolved eco-phenotypes, only unevolved eco-phenotypes or both types of eco-phenotypes, according to different classes of effective number of eco-phenotypes. The dashed line corresponds to a fold-increase of 1, i.e. no increase in median significance of neutrality tests based on temporal differentiation. (**Bottom panels**) Fold-increase in median F_{ST} values for SNPs that hit only evolved eco-phenotypes, only unevolved eco-phenotypes or both types of eco-phenotypes, according to different classes of N_{eff} (median F_{ST} across the genome = 0.00293). Significance against a null distribution obtained by bootstrapping: *0.05 > P > 0.01, **0.01 > P > 0.001, ***P < 0.001, ns: non-significant.

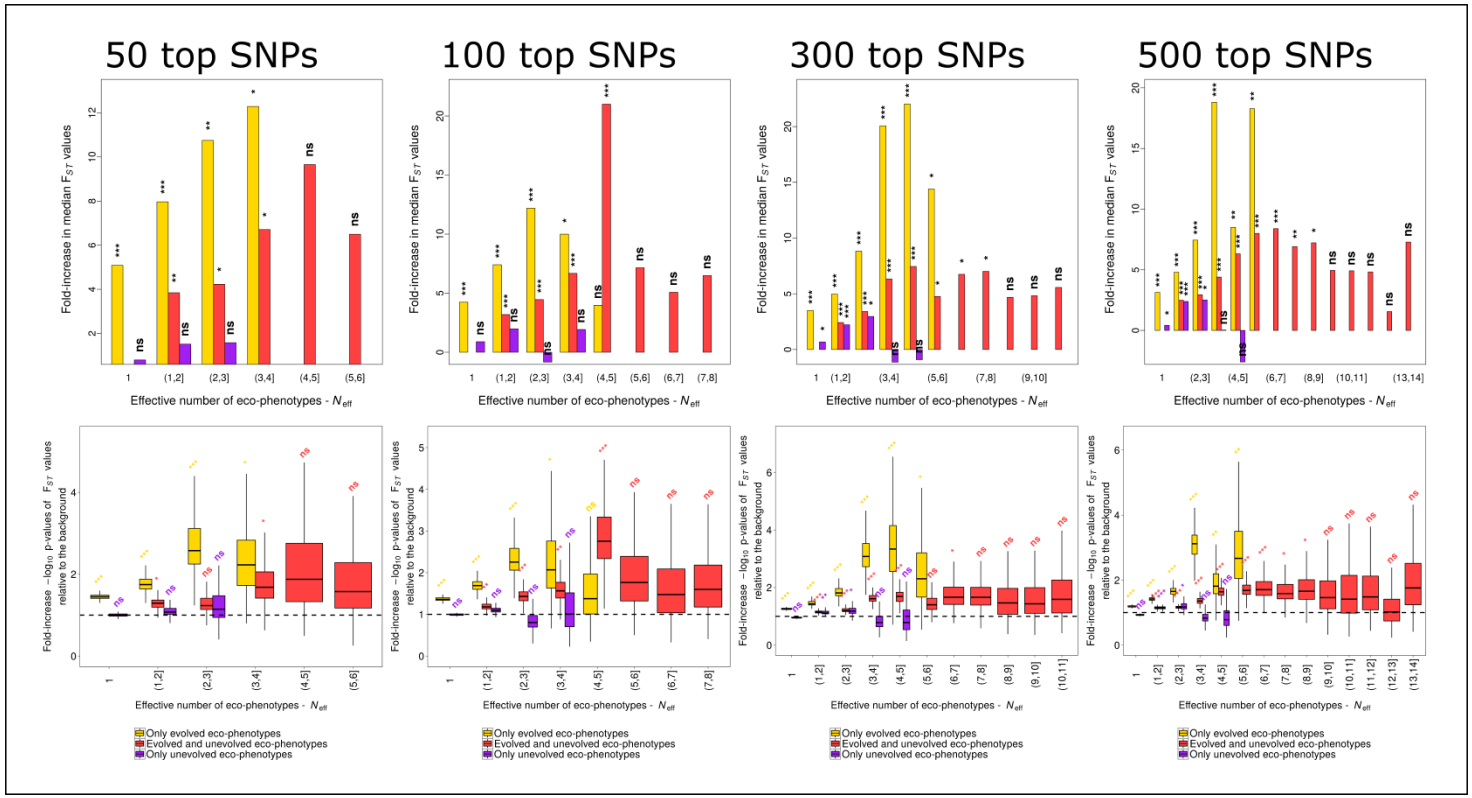

Figure S13C | Degree of pleiotropy and pleiotropic scaling in the TOU-A population when considering SNPs with a –log$_{10}$ *p*-value above 6, 5 and 4. (**Top panels**) Frequency distribution of the effective number of eco-phenotypes affected by a SNP (N_{eff}, accounting for the correlations between eco-phenotypes) among the 21,268 unique top SNPs. (**Bottom panels**) Regression of total effect size T_M (total effect size by the Manhattan distance) on N_{eff}. The formula corresponds to the pleiotropic scaling relationship $\boldsymbol{T_M = c^* N_{eff}^{\ d}}$. A scaling component d exceeding 1 indicates that the mean per-trait effect size of a given top SNP increased with N_{eff}[8]. Solid red line: fitted relationship between T_M and N_{eff}, solid black line: linear dependence ($d = 1$).

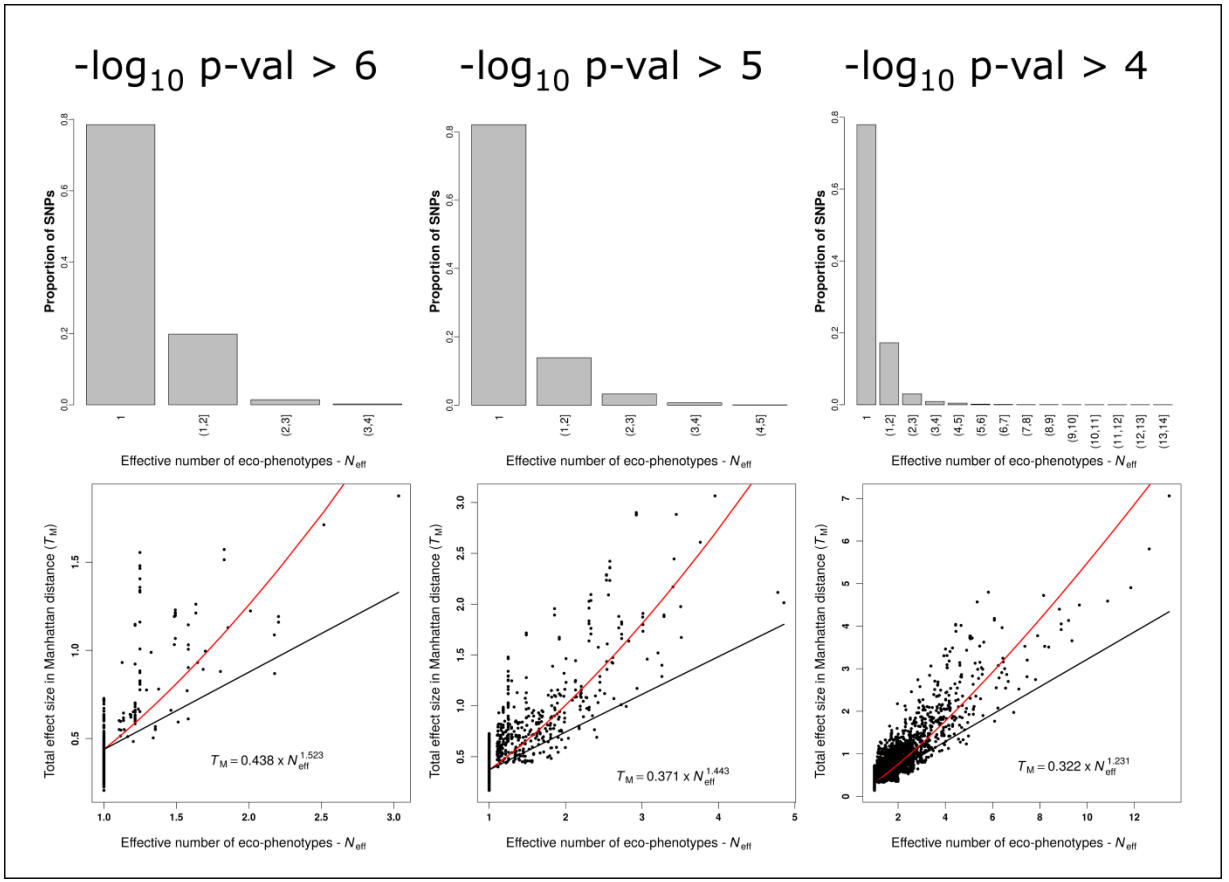

Figure S13D | Significance and strength of selection in the TOU-A population when SNPs with a $-\log_{10}$ *p*-value above 6, 5 and 4. (**Top panels**) Fold-increase in median $-\log_{10}$ (*p*-values) of neutrality tests based on temporal differentiation for SNPs that hit only evolved eco-phenotypes, only unevolved eco-phenotypes or both types of eco-phenotypes, according to different classes of effective number of eco-phenotypes. The dashed line corresponds to a fold-increase of 1, i.e. no increase in median significance of neutrality tests based on temporal differentiation. (**Bottom panels**) Fold-increase in median F_{ST} values for SNPs that hit only evolved eco-phenotypes, only unevolved eco-phenotypes or both types of eco-phenotypes, according to different classes of N_{eff} (median F_{ST} across the genome = 0.00293). Significance against a null distribution obtained by bootstrapping: *0.05 > *P* > 0.01, **0.01 > *P* > 0.001, ***$P < 0.001$, ns: non-significant.

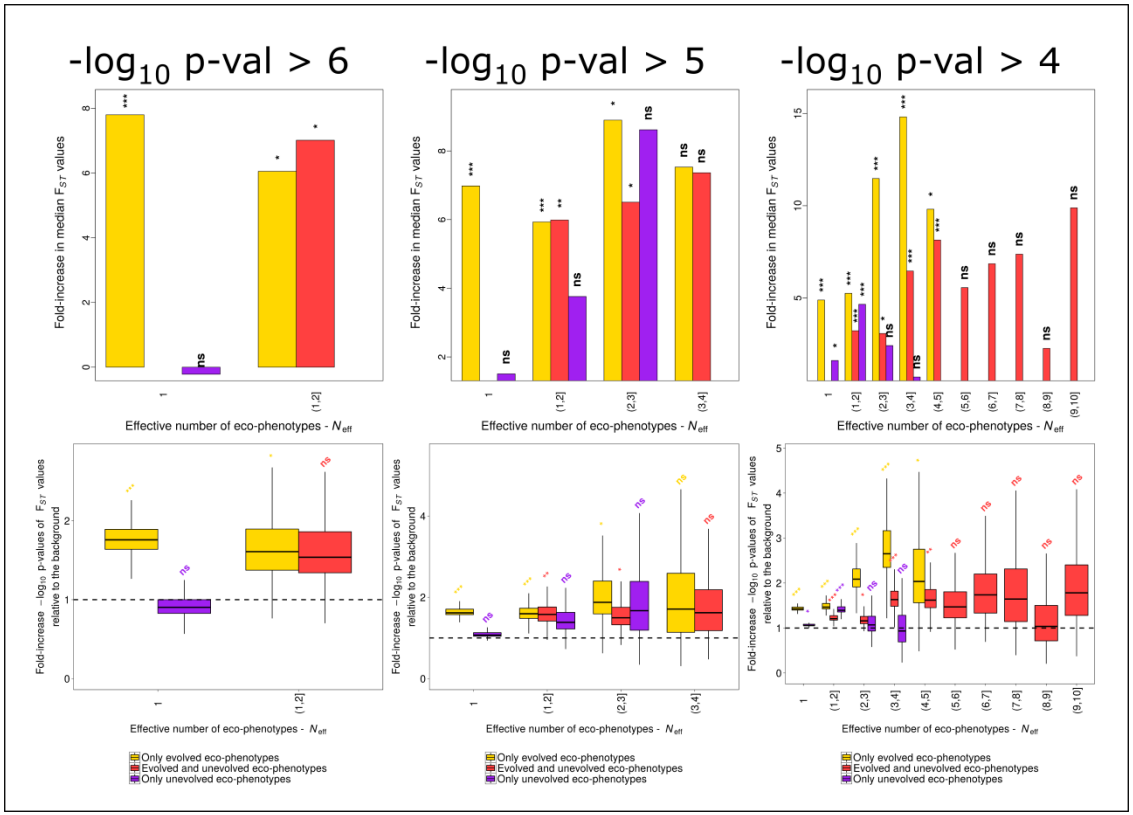

Figure S14 | Partitioning of pleiotropic SNPs associated either with evolved eco-phenotypes or with unevolved eco-phenotypes, according to three types of pleiotropy. N_{eff}: effective number of eco-phenotypes.

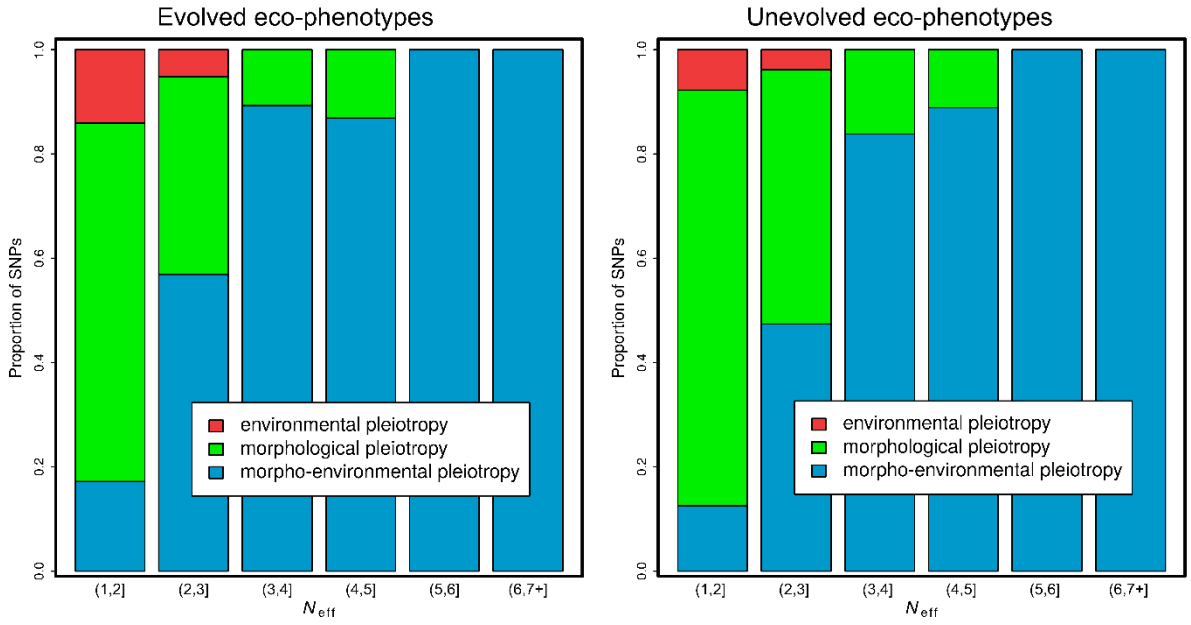

Figure S15 | Scaling relationships between total phenotypic effect size of the 200 top SNPs and the number of eco-phenotypes (*N*, left panels) or the effective number of eco-phenotypes (N_{eff}, right panels). The pleiotropic scaling relationship was calculated as (i) $T_M = c^* {N_{eff}}^d$, with T_M corresponding to the Manhattan distance (bottom panels) and (ii) $T_E = a^* Neff^b$, with T_E corresponding to the Euclidean distance (top panels).

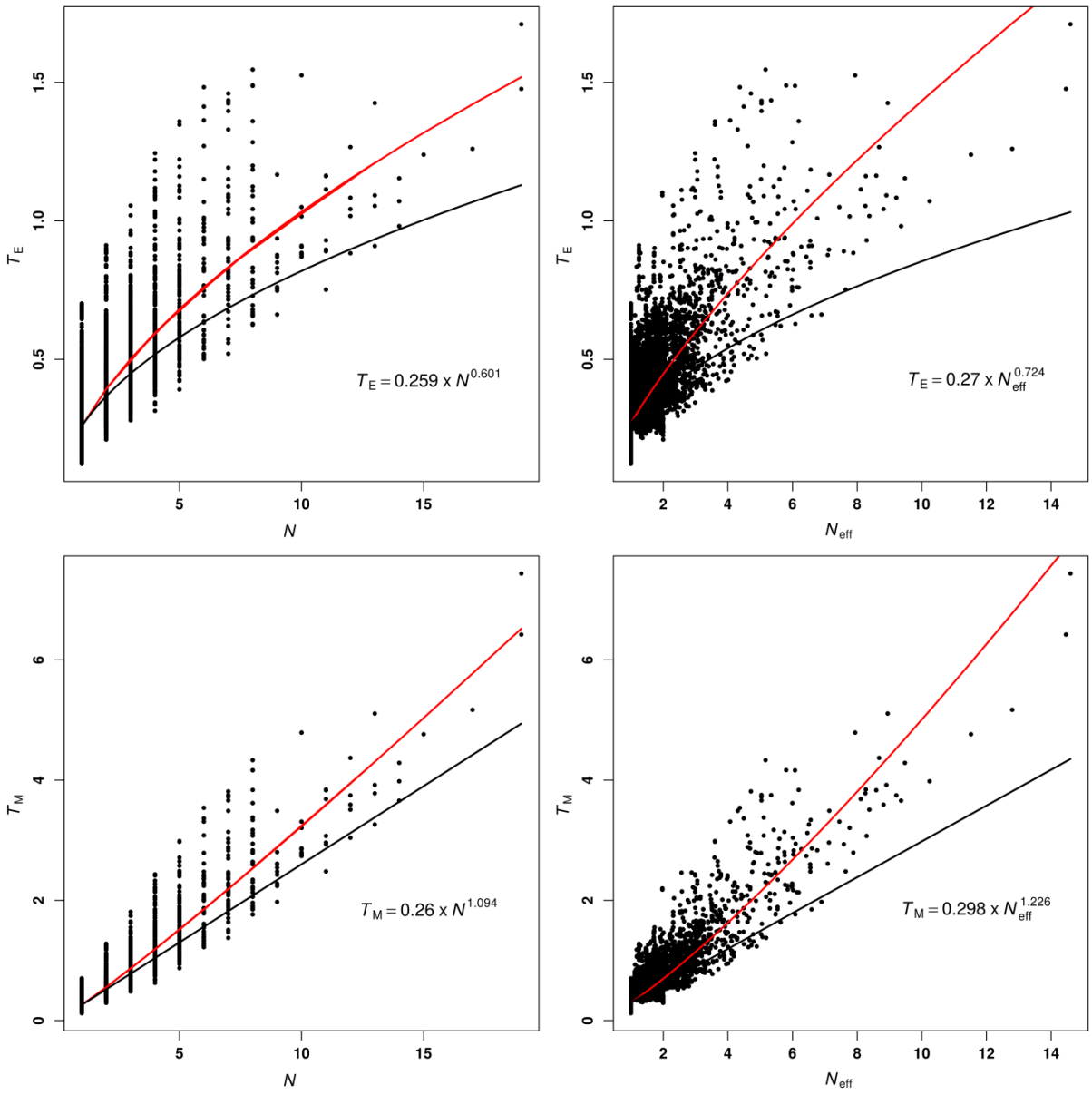

Figure S16 | Genome-wide scan for selection based on temporal differentiation. (**a**) Manhattan plot of F_{ST} at each SNP marker (dots) along the *A. thaliana* genome. The blue dashed line corresponds to the 0.1% upper tail of the F_{ST} value distribution (n = 982). Median F_{ST} across the genome = 0.00293. (**b**) -$\log_{10}$ (*p*-value) of the simulation-based test of the null hypothesis that the locus-specific differentiation measured at each SNP is only due to genetic drift. Only SNP markers with MARF > 7% are considered.

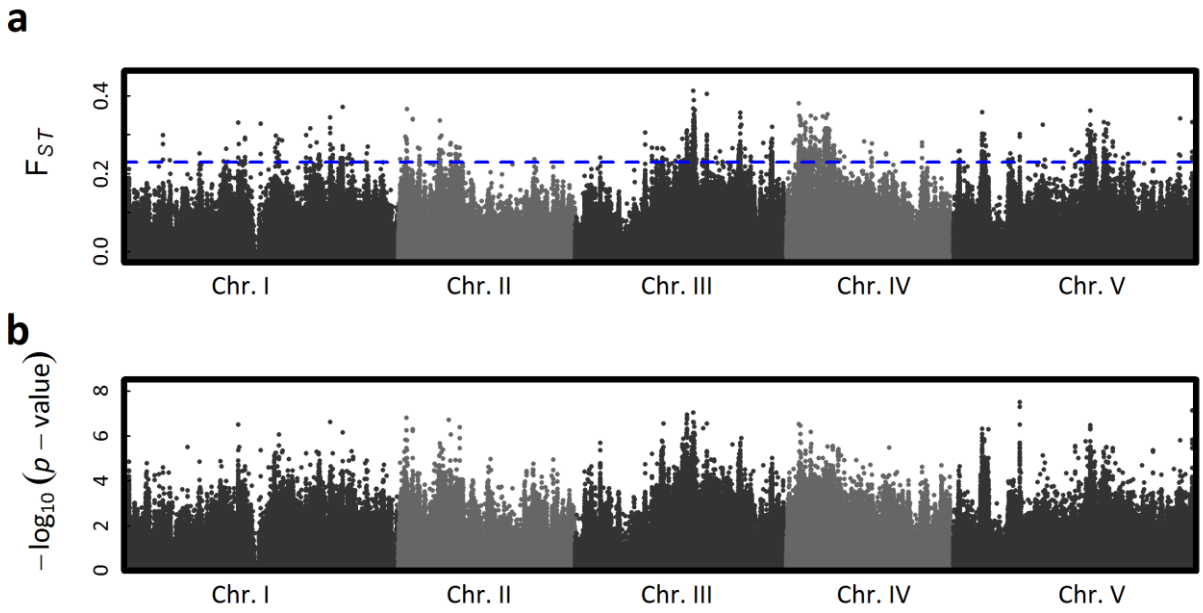

Figure S17 | Polarity of effects. (**a**) Proportion of top SNPs associated with evolved eco-phenotypes with a polarity of effects in line with the direction of phenotypic evolution, according to different classes of N_{eff}. (**b**) Effect of polarity effects on the fold-increase in median F_{ST} values for SNPs that hit only evolved eco-phenotypes, according to different classes of N_{eff} (median F_{ST} across the genome = 0.00293). Significance against a null distribution obtained by bootstrapping: *0.05 > P > 0.01, **0.01 > P > 0.001, ***P < 0.001, absence of symbols: non-significant. Due to the small number of SNPs with an effective number of eco-phenotypes above 4, those SNPs were grouped for testing the significance of fold-increase in median F_{ST} values.

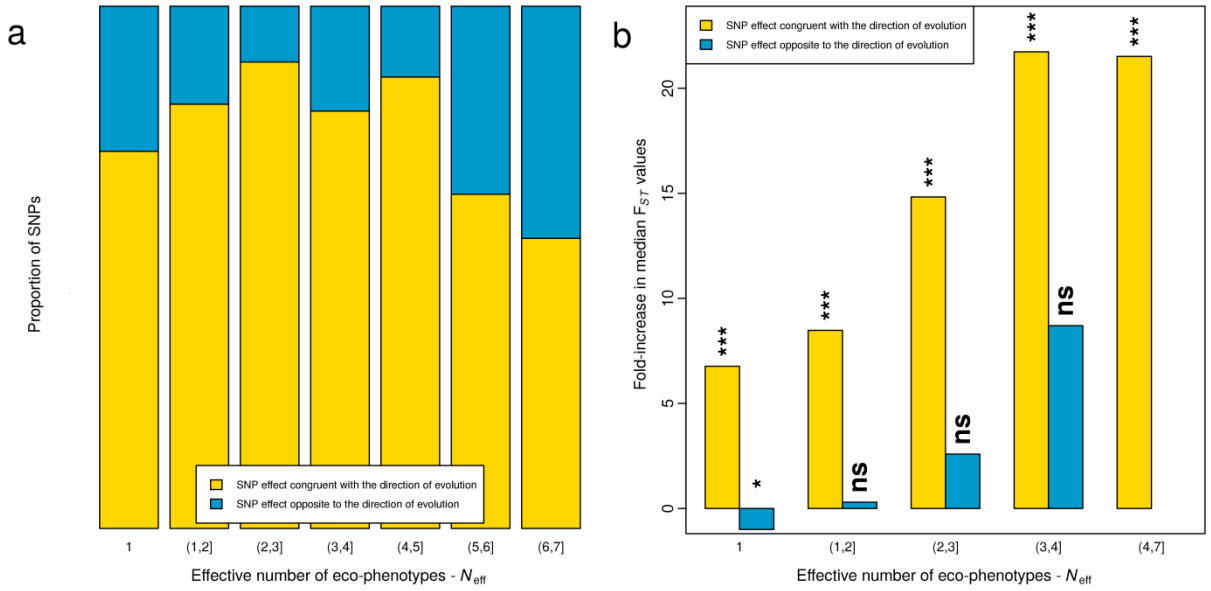

Figure S18 | Relationship between mean of F_{ST} values (based on 200 top SNPs) and absolute estimate of *haldanes* for unevolved eco-phenotypes (n = 68) and evolved eco-phenotypes (n = 74).

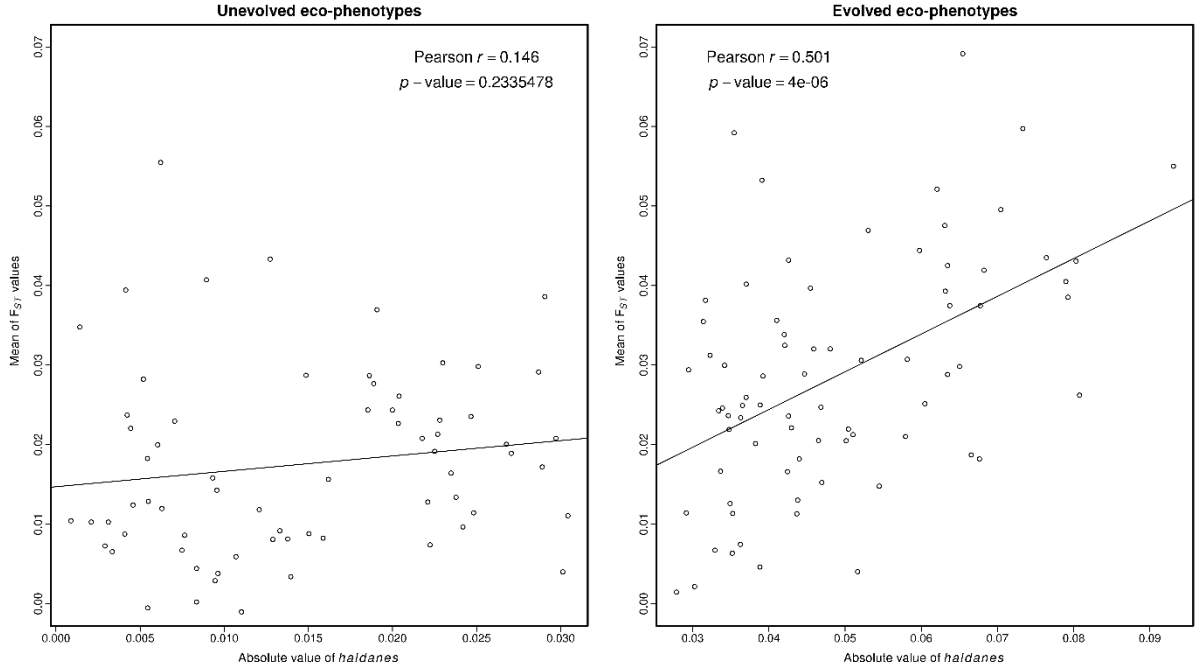

Figure S19 | Evolution between 2002 and 2010 of the proportion of accessions with a rapid (RV) or slow vernalization (SV) response. The two types of vernalization response corresponds to degree of reactivation of *FLC* expression after four weeks of cold[22].

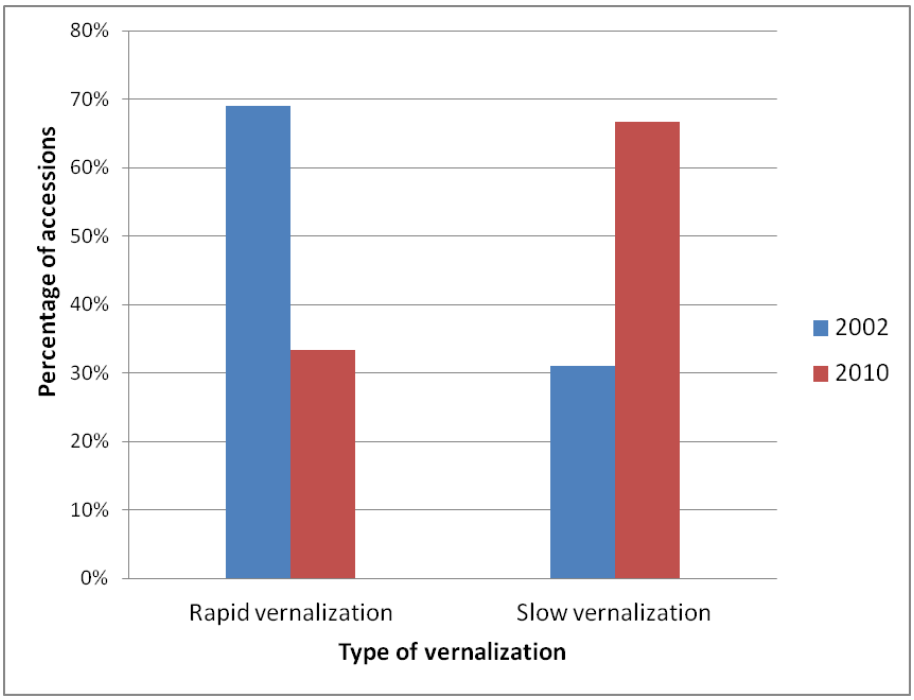

Figure S20 | The distribution dependence of *p*-value distribution on minor allele relative frequency (MARF) for EMMAX across the 144 eco-phenotypes (see Fig. 1). For a given MARF value, each point corresponds to the quantile at 99% of the *p*-value distribution of one of the 144 heritable eco-phenotypes. A locally-weighted polynomial regression is illustrated by a red solid line. A MARF threshold above 7% is depicted by a dashed blue line.

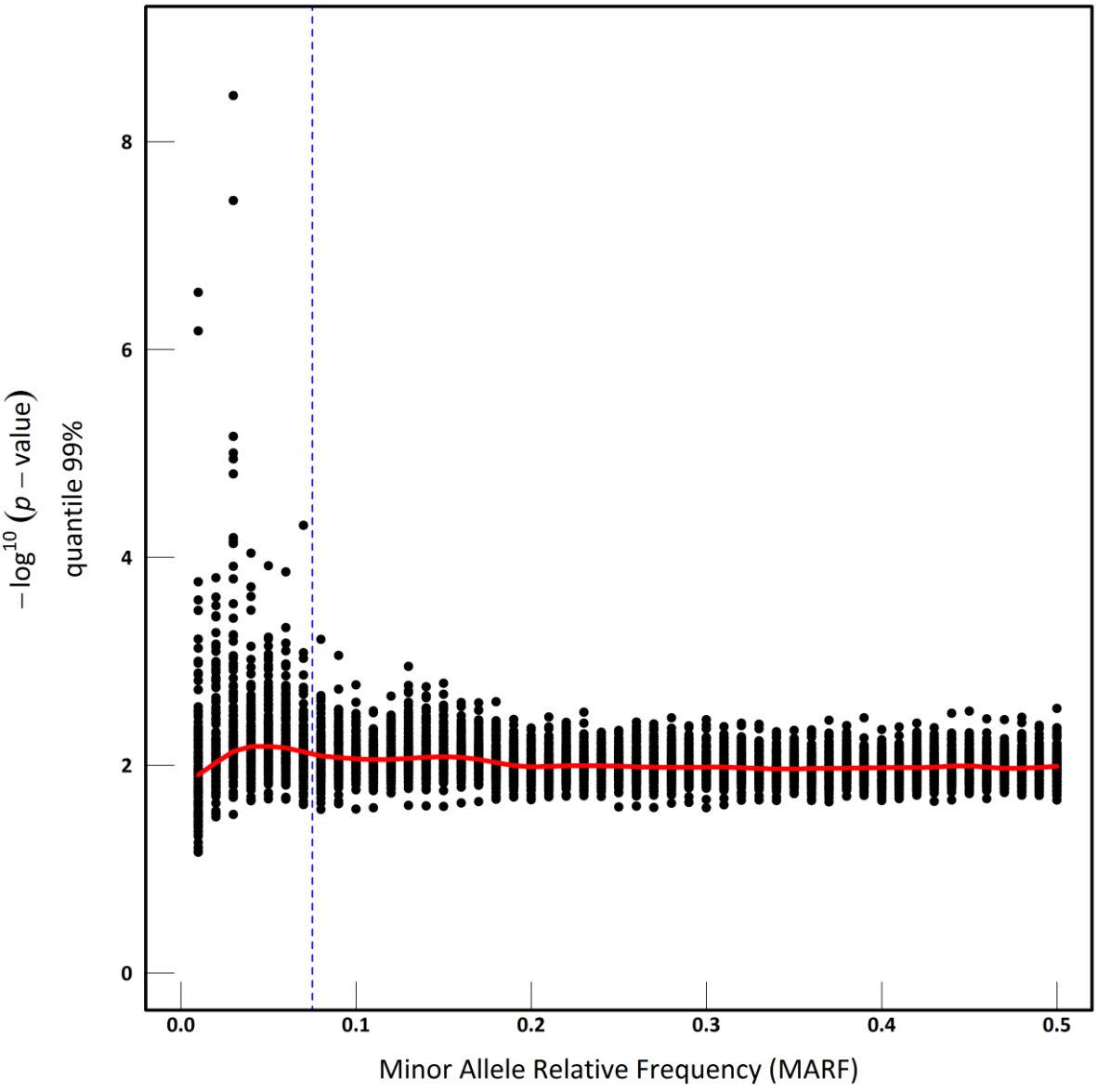

Figure S21 | Distribution of *p*-values associated with temporal F_{ST} estimates for 981,617 SNPS with a MARF > 0.07.

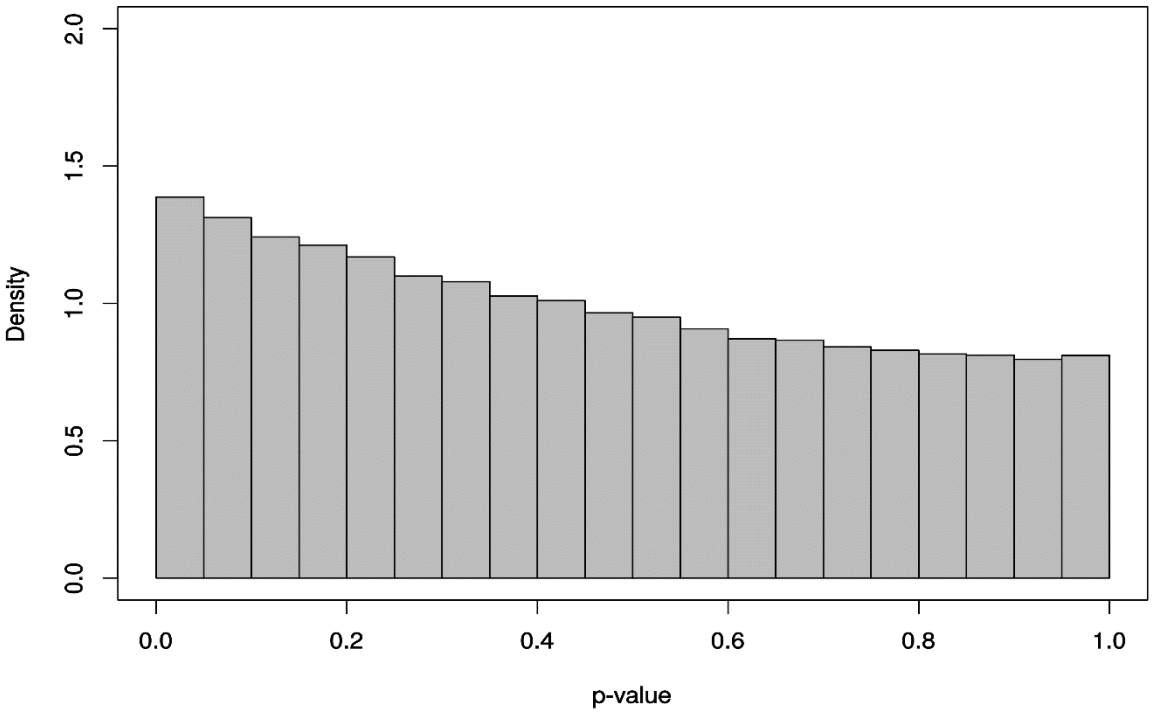

Table S1 | Phenotypic variation of 195 accessions sampled in 2002 and 2010 and scored across six *in situ* 'soil x competition' micro-habitats.

	Model terms§																					
	block (soil*comp)		soil		comp		soil*comp		year		soil*year		comp*year		soil*comp* year		acc (year)		acc(year)* soil		acc(year)* comp		acc(year)* soil* comp	
Traits ǂ	*F*	*P*	*F*	*P*	*F*	*P*	*F*	*P*	*F*	*P*	*F*	*P*	*F*	*P*	*F*	*P*	*LRT*	*P*	*LRT*	*P*	*LRT*	*P*	*LRT*	*P*
GERM	5.40	***	53.44	***	104.47	***	64.64	***	8.61	**	10.13	***	0.51	ns	0.08	ns	299.1	***	0.0	ns	0.0	ns	7.9	*
BT	3.90	***	23.57	***	120.85	***	25.07	***	13.46	**	11.13	***	22.40	***	4.54	***ns***	280.7	***	5.0	*	13.5	**	5.8	***ns***
INT	1.65	*	29.20	***	66.50	***	42.51	***	13.22	**	7.93	**	16.85	***	2.39	ns	140.4	***	0.6	ns	16.1	**	4.1	***ns***
RP	8.24	***	132.02	***	45.37	***	20.95	***	19.18	***	3.65	***ns***	12.60	**	1.62	ns	287.4	***	17.3	***	2.7	ns	0.0	ns
DIAM	5.28	***	75.04	***	57.82	***	46.57	***	0.16	ns	5.34	*	0.11	ns	0.12	ns	40.1	***	2.8	ns	0.0	ns	0.2	ns
H1F	2.41	***	177.58	***	31.60	***	86.96	***	7.29	*	1.41	ns	0.64	ns	2.37	ns	125.5	***	10.7	**	0.8	ns	1.3	ns
HSTEM	4.01	***	342.68	***	14.99	***	55.05	***	0.71	ns	0.08	ns	1.51	ns	2.41	ns	178.0	***	49.9	***	0.2	ns	0.0	ns
HMAX	6.63	***	584.30	***	4.24	***ns***	84.33	***	0.39	ns	0.88	ns	0.17	ns	2.72	ns	162.5	***	43.4	***	0.2	ns	0.0	ns
HD	1.82	*	77.84	***	99.75	***	27.52	***	8.96	**	2.19	ns	2.90	ns	0.89	ns	175.8	***	0.0	ns	0.0	ns	8.9	*
RAMPB_WF	2.73	***	34.20	***	16.26	***	37.44	***	13.43	**	0.20	ns	0.19	ns	3.42	***ns***	47.8	***	6.7	*	7.1	***ns***	0.0	ns
RAMPB_WOF	1.43	ns	2.01	ns	3.89	ns	2.58	ns	0.41	ns	1.88	ns	4.45	***ns***	0.36	ns	53.8	***	1.3	ns	0.0	ns	0.0	ns
TOTPB	2.43	***	53.77	***	13.13	***	48.04	***	12.57	**	1.92	ns	3.18	ns	6.41	*	118.9	***	5.3	*	4.8	***ns***	0.0	ns
RAMBB	2.90	***	9.94	***	120.87	***	14.61	***	3.28	ns	3.00	ns	0.84	ns	0.12	ns	68.2	***	1.9	ns	1.3	ns	0.1	ns
TOTB	3.48	***	42.53	***	113.24	***	49.52	***	1.95	ns	0.35	ns	0.15	ns	1.57	ns	42.3	***	2.1	ns	3.3	ns	0.0	ns
FITTOT	5.07	***	201.80	***	28.37	***	35.21	***	0.29	ns	0.31	ns	0.22	ns	1.61	ns	20.5	***	13.1	**	0.0	ns	0.0	ns
FITSTEM	3.23	***	161.17	***	0.79	ns	14.78	***	7.09	*	0.14	ns	0.46	ns	4.16	***ns***	119.6	***	44.5	***	0.1	ns	0.0	ns
FRUITSTEM	3.01	***	83.92	***	0.49	ns	9.86	***	8.97	**	0.09	ns	0.00	ns	3.18	***ns***	85.6	***	47.9	***	0.1	ns	0.1	ns
SILSTEM	3.76	***	434.03	***	101.02	***	31.50	***	1.78	ns	2.39	ns	2.52	ns	1.96	ns	256.6	***	20.8	***	3.0	ns	0.0	ns
FITPB	3.24	***	197.91	***	0.19	ns	42.05	***	9.71	**	0.99	ns	0.78	ns	8.94	**	25.0	***	4.8	*	0.0	ns	8.1	*
FRUITPB	3.49	***	158.53	***	1.19	ns	45.88	***	10.64	**	0.72	ns	0.01	ns	6.29	*	22.7	***	12.7	**	0.0	ns	2.0	ns
SILPB	3.86	***	450.20	***	33.62	***	25.65	***	0.34	ns	1.11	ns	1.42	ns	4.17	***ns***	211.2	***	8.1	*	0.0	ns	0.0	ns
FITBB	1.82	*	20.38	***	36.04	***	2.59	ns	0.21	ns	2.51	ns	0.23	ns	0.17	ns	7.9	**	1.7	ns	0.0	ns	0.1	ns
FRUITBB	2.81	***	24.36	***	95.10	***	8.08	***	2.16	ns	2.18	ns	0.56	ns	0.14	ns	41.4	***	8.3	*	0.0	ns	0.7	ns
SILBB	2.48	***	148.46	***	12.90	***	16.34	***	0.03	ns	1.91	ns	0.14	ns	2.66	ns	149.6	***	6.0	*	0.0	ns	0.0	ns
RSTEM	3.12	***	76.90	***	34.61	***	19.77	***	0.97	ns	0.09	ns	1.87	ns	0.17	ns	25.9	***	5.7	*	0.3	ns	0.0	ns
RPB	1.61	*	67.83	***	42.64	***	5.22	**	7.69	*	0.56	ns	1.43	ns	4.39	***ns***	55.9	***	6.9	*	0.0	ns	0.2	ns
RBB	1.73	*	19.98	***	27.71	***	0.17	ns	15.53	***	1.14	ns	0.91	ns	0.51	ns	6.0	***ns***	3.3	ns	0.9	ns	0.2	ns
INTERNOD	1.21	ns	32.07	***	1.77	ns	1.10	ns	3.42	ns	0.03	ns	0.00	ns	1.79	ns	2.7	ns	2.0	ns	0.0	ns	0.0	ns
SURVIVAL	39.31	***	57.15	***	0.06	ns	47.30	***	Inf	***	Inf	***	Inf	***	Inf	**	1.0	ns	3.5	ns	0.0	ns	ne	ne

*0.05 > *P* > 0.01, **0.01 > *P* > 0.001, ***$P < 0.001$. ns: non-significant, *ns* : significant before a false discovery rate (FDR) correction at the nominal level of 5%, ne: not estimated.

ǂ All traits were measured quantitatively with the exception of survival which is a binary trait. § Each trait was modeled separately using a mixed model. Model random terms were tested with likelihood ratio tests (LRT) of models with and without these effects. A correction for the number of tests was performed for each modeled effect (*i.e.* per column) to control the FDR at a nominal level of 5%.

Table S2 | Broad-sense heritability values (H^2) of the 174 eco-phenotypes scored across six *in situ* 'soil x competition' micro-habitats. *P*: bold values indicate significant broad-sense heritability estimates after a false discovery rate (FDR) correction at the nominal level of 5%.

Ecophenotype	H^2	*P*
BT_A_wo_P	0.868	**0.00E+00**
BT_A_w_P	0.847	**0.00E+00**
BT_B_wo_P	0.864	**0.00E+00**
BT_B_w_P	0.827	**0.00E+00**
BT_C_wo_P	0.864	**0.00E+00**
BT_C_w_P	0.843	**0.00E+00**
DIAM_A_wo_P	0.084	6.27E-01
DIAM_A_w_P	0.480	**4.50E-08**
DIAM_B_wo_P	0.329	**1.01E-03**
DIAM_B_w_P	0.303	**4.90E-03**
DIAM_C_wo_P	0.174	1.38E-01
DIAM_C_w_P	0.470	**5.40E-08**
FITBB_A_wo_P	0.261	2.64E-01
FITBB_A_w_P	0.005	1.00E+00
FITBB_B_wo_P	0.256	1.69E-01
FITBB_B_w_P	0.260	1.60E-01
FITBB_C_wo_P	0.323	8.22E-02
FITBB_C_w_P	0.451	**2.21E-03**
FITPB_A_wo_P	0.442	**3.14E-04**
FITPB_A_w_P	0.398	**3.84E-04**
FITPB_B_wo_P	0.341	**2.06E-03**
FITPB_B_w_P	0.174	1.93E-01
FITPB_C_wo_P	0.490	**1.05E-06**
FITPB_C_w_P	0.602	**1.51E-12**
FITSTEM_A_wo_P	0.626	**2.07E-11**
FITSTEM_A_w_P	0.644	**3.58E-16**
FITSTEM_B_wo_P	0.495	**3.65E-08**
FITSTEM_B_w_P	0.419	**2.80E-05**
FITSTEM_C_wo_P	0.709	**0.00E+00**
FITSTEM_C_w_P	0.716	**0.00E+00**
FITTOT_A_wo_P	0.230	7.29E-02
FITTOT_A_w_P	0.399	**6.65E-04**
FITTOT_B_wo_P	0.170	1.86E-01
FITTOT_B_w_P	0.202	**2.89E-02**
FITTOT_C_wo_P	0.418	**2.63E-02**
FITTOT_C_w_P	0.566	**8.90E-07**
FRUITBB_A_wo_P	0.256	5.33E-02
FRUITBB_A_w_P	0.342	**6.65E-04**
FRUITBB_B_wo_P	0.334	**2.20E-03**
FRUITBB_B_w_P	0.400	**5.20E-05**
FRUITBB_C_wo_P	0.303	**6.05E-03**
FRUITBB_C_w_P	0.635	**0.00E+00**
FRUITPB_A_wo_P	0.326	**8.95E-03**
FRUITPB_A_w_P	0.401	**4.18E-05**
FRUITPB_B_wo_P	0.252	**2.21E-02**
FRUITPB_B_w_P	0.147	2.45E-01
FRUITPB_C_wo_P	0.447	**2.94E-06**
FRUITPB_C_w_P	0.591	**7.08E-15**

Ecophenotype	H^2	*P*
FRUITSTEM_A_wo_P	0.515	**1.53E-07**
FRUITSTEM_A_w_P	0.601	**2.61E-14**
FRUITSTEM_B_wo_P	0.370	**3.27E-04**
FRUITSTEM_B_w_P	0.323	**3.51E-03**
FRUITSTEM_C_wo_P	0.676	**0.00E+00**
FRUITSTEM_C_w_P	0.749	**0.00E+00**
GERM_A_wo_P	0.827	**0.00E+00**
GERM_A_w_P	0.796	**0.00E+00**
GERM_B_wo_P	0.781	**0.00E+00**
GERM_B_w_P	0.773	**0.00E+00**
GERM_C_wo_P	0.659	**0.00E+00**
GERM_C_w_P	0.738	**0.00E+00**
H1F_A_wo_P	0.536	**6.72E-09**
H1F_A_w_P	0.567	**4.27E-12**
H1F_B_wo_P	0.705	**0.00E+00**
H1F_B_w_P	0.541	**2.66E-09**
H1F_C_wo_P	0.574	**6.09E-12**
H1F_C_w_P	0.695	**0.00E+00**
HD_A_wo_P	0.518	**1.10E-07**
HD_A_w_P	0.673	**0.00E+00**
HD_B_wo_P	0.728	**0.00E+00**
HD_B_w_P	0.666	**0.00E+00**
HD_C_wo_P	0.529	**1.80E-09**
HD_C_w_P	0.714	**0.00E+00**
HMAX_A_wo_P	0.607	**2.19E-12**
HMAX_A_w_P	0.627	**0.00E+00**
HMAX_B_wo_P	0.625	**0.00E+00**
HMAX_B_w_P	0.574	**1.30E-11**
HMAX_C_wo_P	0.725	**0.00E+00**
HMAX_C_w_P	0.720	**0.00E+00**
HSTEM_A_wo_P	0.615	**2.30E-12**
HSTEM_A_w_P	0.640	**0.00E+00**
HSTEM_B_wo_P	0.620	**0.00E+00**
HSTEM_B_w_P	0.614	**1.25E-14**
HSTEM_C_wo_P	0.748	**0.00E+00**
HSTEM_C_w_P	0.761	**0.00E+00**
INT_A_wo_P	0.755	**0.00E+00**
INT_A_w_P	0.641	**0.00E+00**
INT_B_wo_P	0.771	**0.00E+00**
INT_B_w_P	0.623	**0.00E+00**
INT_C_wo_P	0.720	**0.00E+00**
INT_C_w_P	0.513	**4.52E-10**
INTERNOD_A_wo_P	0.026	1.00E+00
INTERNOD_A_w_P	0.103	5.66E-01
INTERNOD_B_wo_P	0.595	**1.73E-14**
INTERNOD_B_w_P	0.472	**9.37E-07**
INTERNOD_C_wo_P	0.105	4.71E-01
INTERNOD_C_w_P	0.160	1.00E+00

Table S2 (continued)

Ecophenotype	H^2	*P*
RAMBB_A_wo_P	0.316	**1.19E-02**
RAMBB_A_w_P	0.343	**6.65E-04**
RAMBB_B_wo_P	0.464	**9.28E-07**
RAMBB_B_w_P	0.388	**1.73E-04**
RAMBB_C_wo_P	0.344	**1.25E-03**
RAMBB_C_w_P	0.669	**0.00E+00**
RAMPB_WOF_A_wo_P	0.314	**8.95E-03**
RAMPB_WOF_A_w_P	0.555	**1.17E-11**
RAMPB_WOF_B_wo_P	0.182	1.54E-01
RAMPB_WOF_B_w_P	0.305	**5.83E-03**
RAMPB_WOF_C_wo_P	0.152	2.14E-01
RAMPB_WOF_C_w_P	0.405	**1.95E-05**
RAMPB_WF_A_wo_P	0.493	**8.70E-07**
RAMPB_WF_A_w_P	0.438	**2.94E-06**
RAMPB_WF_B_wo_P	0.484	**1.18E-07**
RAMPB_WF_B_w_P	0.398	**2.14E-04**
RAMPB_WF_C_wo_P	0.349	**9.08E-04**
RAMPB_WF_C_w_P	0.497	**1.09E-08**
RBB_A_wo_P	0.398	1.95E-01
RBB_A_w_P	0.440	1.05E-01
RBB_B_wo_P	0.520	**3.27E-04**
RBB_B_w_P	0.607	**1.90E-06**
RBB_C_wo_P	0.299	1.60E-01
RBB_C_w_P	0.664	**3.17E-05**
RP_A_wo_P	0.801	**0.00E+00**
RP_A_w_P	0.827	**0.00E+00**
RP_B_wo_P	0.798	**0.00E+00**
RP_B_w_P	0.742	**0.00E+00**
RP_C_wo_P	0.842	**0.00E+00**
RP_C_w_P	0.817	**0.00E+00**
RPB_A_wo_P	0.403	**2.81E-03**
RPB_A_w_P	0.345	**2.23E-03**
RPB_B_wo_P	0.555	**4.52E-10**
RPB_B_w_P	0.430	**1.65E-04**
RPB_C_wo_P	0.255	**1.56E-02**
RPB_C_w_P	0.505	**1.09E-08**
RSTEM_A_wo_P	0.253	7.42E-02
RSTEM_A_w_P	0.369	**1.43E-03**
RSTEM_B_wo_P	0.355	**5.97E-03**
RSTEM_B_w_P	0.293	**1.61E-02**
RSTEM_C_wo_P	0.074	1.00E+00
RSTEM_C_w_P	0.405	**3.47E-04**
SILBB_A_wo_P	0.677	**2.55E-06**
SILBB_A_w_P	0.681	**3.64E-04**
SILBB_B_wo_P	0.803	**0.00E+00**
SILBB_B_w_P	0.718	**2.63E-07**
SILBB_C_wo_P	0.713	**1.40E-11**
SILBB_C_w_P	0.729	**2.45E-10**

Ecophenotype	H^2	*P*
SILPB_A_wo_P	0.638	**3.52E-12**
SILPB_A_w_P	0.604	**9.79E-12**
SILPB_B_wo_P	0.779	**0.00E+00**
SILPB_B_w_P	0.702	**0.00E+00**
SILPB_C_wo_P	0.635	**8.41E-14**
SILPB_C_w_P	0.725	**0.00E+00**
SILSTEM_A_wo_P	0.774	**0.00E+00**
SILSTEM_A_w_P	0.781	**0.00E+00**
SILSTEM_B_wo_P	0.797	**0.00E+00**
SILSTEM_B_w_P	0.797	**0.00E+00**
SILSTEM_C_wo_P	0.743	**0.00E+00**
SILSTEM_C_w_P	0.755	**0.00E+00**
SURVIVAL_A_wo_P	0.022	8.72E-01
SURVIVAL_A_w_P	0.000	1.00E+00
SURVIVAL_B_wo_P	0.135	2.02E-01
SURVIVAL_B_w_P	0.113	2.90E-01
SURVIVAL_C_wo_P	0.000	1.00E+00
SURVIVAL_C_w_P	0.227	**2.29E-02**
TOTB_A_wo_P	0.359	**2.53E-03**
TOTB_A_w_P	0.216	6.31E-02
TOTB_B_wo_P	0.372	**4.52E-04**
TOTB_B_w_P	0.175	1.75E-01
TOTB_C_wo_P	0.254	**2.65E-02**
TOTB_C_w_P	0.542	**6.87E-11**
TOTPB_A_wo_P	0.565	**7.37E-10**
TOTPB_A_w_P	0.498	**3.19E-08**
TOTPB_B_wo_P	0.668	**0.00E+00**
TOTPB_B_w_P	0.580	**1.30E-11**
TOTPB_C_wo_P	0.525	**6.60E-10**
TOTPB_C_w_P	0.618	**4.60E-16**

Table S3 | Manhattan distance: scaling relationships between total phenotypic effect size of SNPs with the highest association and the effective number of eco-phenotypes (N_{eff}). The pleiotropic scaling relationship between the total effect size and the effective number of eco-phenotypes was calculated as $T_M = c^* {N_{eff}}^d$, with T_M corresponding to the Manhattan distance and calculated as $T_M = \sum_{i=1}^{n} |A_i|$, where n is the degree of pleiotropy and A_i is the standardized allelic effect. To avoid pseudo-replication due to the presence of several top SNPs in a given LD block, the pleiotropic scaling was also calculated for each threshold number of top SNPs and each threshold of significance, (i) by considering the mean value of the total effect size and N_{eff} per LD block containing top SNPs ('Mean per block' column) and (ii) by randomly sampling one top SNP per LD block (this step was repeated 1,000 times) ('Random' column).

T_M	Threshold	Total SNPs	Unique SNPs	% pleiotropic SNPs	All unique SNPs		Mean per block		Random	
					c	d	c	d	c	d
number of top SNPs	50 SNPs	7200	5728	16.69	0.320	1.254	0.317	1.300	0.320 (0.315 - 0.324)	1.268 (1.224 - 1.323)
	100 SNPs	14400	11100	19.05	0.311	1.241	0.309	1.275	0.311 (0.307 - 0.316)	1.253 (1.214 - 1.294)
	200 SNPs	28800	21268	21.86	0.298	1.226	0.295	1.255	0.296 (0.292 - 0.300)	1.243 (1.208 - 1.274)
	300 SNPs	43200	30854	24.40	0.289	1.212	0.289	1.223	0.289 (0.285 - 0.293)	1.217 (1.187 - 1.249)
	500 SNPs	72000	48851	27.64	0.280	1.188	0.283	1.178	0.282 (0.278 - 0.287)	1.181 (1.152 - 1.204)
$-\log_{10} p$-value	> 6	538	424	21.46	0.438	1.523	0.423	1.799	0.425 (0.416 - 0.438)	1.736 (1.503 - 1.920)
	> 5	3165	2457	17.91	0.363	1.518	0.361	1.510	0.362 (0.350 - 0.372)	1.490 (1.382 - 1.637)
	> 4	22822	16720	22.06	0.322	1.231	0.318	1.267	0.320 (0.314 - 0.326)	1.241 (1.197 - 1.293)

Table S4 | Euclidean distance: scaling relationships between total phenotypic effect size of SNPs with the highest association and the effective number of eco-phenotypes (N_{eff}). The pleiotropic scaling relationship between the total effect size and the effective number of eco-phenotypes was calculated as $T_E = a^* Neff^b$, with T_E corresponding to the Euclidean distance and calculated as $T_E = \sqrt{\sum_{i=1}^{n} A_i^2}$, where n is the degree of pleiotropy and A_i is the standardized allelic effect. To avoid pseudo-replication due to the presence of several top SNPs in a given LD block, the pleiotropic scaling was also calculated for each threshold number of top SNPs and each threshold of significance, (i) by considering the mean value of the total effect size and N_{eff} per LD block containing top SNPs ('Mean per block' column) and (ii) by randomly sampling one top SNP per LD block (this step was repeated 1,000 times) ('Random' column).

T_E	Threshold	Total SNPs	Unique SNPs	% pleiotropic SNPs	All unique SNPs		Mean per block		Random	
					a	b	a	b	a	b
number of top SNPs	50	7200	5728	16.69	0.296	0.735	0.295	0.766	0.296 (0.294 - 0.298)	0.757 (0.718 - 0.803)
	100	14400	11100	19.05	0.283	0.741	0.283	0.771	0.284 (0.282 - 0.286)	0.764 (0.729 - 0.797)
	200	28800	21268	21.86	0.270	0.724	0.268	0.751	0.269 (0.267 - 0.271)	0.747 (0.722 - 0.772)
	300	43200	30854	24.40	0.263	0.709	0.260	0.728	0.261 (0.259 - 0.263)	0.730 (0.705 - 0.755)
	500	72000	48851	27.64	0.252	0.689	0.250	0.697	0.252 (0.250 - 0.253)	0.705 (0.682 - 0.725)
$-\log_{10} p$-value	> 6	538	424	21.46	0.405	0.888	0.393	1.158	0.395 (0.390 - 0.401)	1.104 (0.884 - 1.285)
	> 5	3165	2457	17.91	0.347	0.825	0.335	0.917	0.335 (0.331 - 0.339)	0.906 (0.835 - 0.990)
	> 4	22822	16720	22.06	0.291	0.722	0.288	0.743	0.290 (0.288 - 0.292)	0.740 (0.706 - 0.776)

Table S5 | Scaling relationships between total phenotypic effect size of the 200 SNPs and the effective number of eco-phenotypes (N_{eff}) according to different N_{eff} cutoffs. $T_M = c^* {N_{eff}}^d$, with T_M corresponding to the Manhattan distance and calculated as $T_M = \sum_{i=1}^{n} |A_i|$, where n is the degree of pleiotropy and A_i is the standardized allelic effect. $T_E = a^* Neff^b$, with T_E corresponding to the Euclidean distance and calculated as $T_E = \sqrt{\sum_{i=1}^{n} A_i^2}$, where n is the degree of pleiotropy and A_i is the standardized allelic effect.

	T_M		T_E	
***Neff* cutoff**	**c**	**d**	**a**	**b**
All SNPs	0.298	1.226	0.270	0.724
10	0.294	1.254	0.270	0.735
8	0.291	1.278	0.269	0.747
6	0.287	1.321	0.268	0.767
4	0.282	1.382	0.267	0.791
3	0.280	1.425	0.267	0.805

Table S6 | List of candidate genes associated with 11 or more evolved eco-phenotypes.

Atg number	no eco-phenotypes	Locus name	Molecular function
AT4G01820	17	ABCB3	member of MDR subfamily
AT4G01830	11	PGP5	P-glycoprotein 5 (PGP5)
AT4G14660	12	NRPE7	Non-catalytic subunit specific to DNA-directed RNA polymerase V
AT4G18350	12	NCED2	Encodes 9-*cis* -epoxycarotenoid dioxygenase, a key enzyme in the biosynthesis of abscisic acid.
AT4G19960	24	AtKUP/HAK/KT9	Encodes a potassium ion transmembrane transporter.
AT4G20325	12		unknown
AT4G20330	11		Transcription initiation factor TFIIE, beta subunit
AT4G20340	13		Transcription factor TFIIE, alpha subunit
AT4G20350	18		oxidoreductases
AT4G20362	15	SORF6	Potential natural antisense gene, locus overlaps with AT4G20360
AT4G20370	11	TSF	Encodes a floral inducer that is a homolog of FT.
AT4G24520	12	ATR1	Encodes a cyp450 reductase likely to be involved in phenylpropanoid metabolism.
AT5G12430	14	TPR16	Encodes one of the 36 carboxylate clamp (CC)-tetratricopeptide repeat (TPR) proteins
AT5G43430	13	ETFBETA	Encodes the electron transfer flavoprotein ETF beta, a putative subunit of the mitochondrial electron transfer flavoprotein complex

Table S7 | Enrichment of biological process in the 0.1% tail of the F_{ST} values.

Biological process	Enrichment	*P* value	Atg number	Locus name	Molecular function	Associated eco-phenotypes[1]
vernalization response	22	**	AT5G10140	*FLC*	MADS-box protein	
			AT4G16845	*VRN2*	nuclear-localized zinc finger protein	H1F_B_w_P, RSTEM_B_wo_P, SURVIVAL_C_w_P, DIAM_B_wo_P, H1F_C_wo_P, SILBB_B_w_P, FITTOT_C_wo_P
regulation of circadian rhythm	21	**	AT5G10140	*FLC*	MADS-box protein	
response to temperature stimulus	21	**	AT5G10140	*FLC*	MADS-box protein	
negative regulation of flower development	21	*	AT5G10140	*FLC*	MADS-box protein	
regulation of cell shape	17	*	AT3G59100	*GLUCAN SYNTHASE-LIKE 11*	protein similar to callose synthase	
			AT4G03550	*POWDERY MILDEW RESISTANT 4*	callose synthase	FRUITSTEM_C_w_P, SILPB_A_wo_P
beta-D-glucan biosynthetic process	17	*	AT3G59100	*GLUCAN SYNTHASE-LIKE 11*	protein similar to callose synthase	
			AT4G03550	*POWDERY MILDEW RESISTANT 4*	callose synthase	FRUITSTEM_C_w_P, SILPB_A_wo_P
pollen tube development	15	*	AT4G05450	*MFDX1*	mitochondrial ferredoxin 1	FRUITSTEM_C_w_P, SILPB_A_wo_P
electron transport chain	15	*	AT4G05450	*MFDX1*	mitochondrial ferredoxin 1	FRUITSTEM_C_w_P, SILPB_A_wo_P
polar nucleus fusion	14	*	AT4G05440	*EMBRYO SAC DEVELOPMENT ARREST 35*	unknown	FRUITSTEM_C_w_P, SILPB_A_wo_P
			AT5G42020	*BIP2*	luminal binding protein	DIAM_C_w_P, TOT_B_C_w_P, RAMPB_WF_C_w_P
stamen development	14	*	AT4G03190	*AFB1*	F box protein belonging to the TIR1 subfamily	
			AT5G41700	*UBIQUITIN CONJUGATING ENZYME 8*	one of the polypeptides that constitute the ubiquitin-conjugating enzyme E2	FITTOT_C_w_P, FRUITPB_C_w_P, RSTEM_B_w_P, SILPB_C_w_P, INT_B_wo_P, SILSTEM_B_wo_P, RAMPB_WF_C_w_P
defense response by callose deposition in cell wall	14	*	AT4G03550	*POWDERY MILDEW RESISTANT 4*	callose synthase	FRUITSTEM_C_w_P, SILPB_A_wo_P
salicylic acid mediated signaling pathway	14	*	AT4G03550	*POWDERY MILDEW RESISTANT 4*	callose synthase	FRUITSTEM_C_w_P, SILPB_A_wo_P
defense response signaling pathway, resistance gene-dependent	14	*	AT4G03550	*POWDERY MILDEW RESISTANT 4*	callose synthase	FRUITSTEM_C_w_P, SILPB_A_wo_P
cell cycle arrest	13	*	AT4G05440	*EMBRYO SAC DEVELOPMENT ARREST 35*	unknown	FRUITSTEM_C_w_P, SILPB_A_wo_P
calcium-mediated signaling	12	*	AT4G03560	*TPC1*	depolarization-activated Ca(2+) channel	
trehalose biosynthetic process	12	*	AT5G10100	*TPPI*	haloacid dehalogenase-like hydrolase (HAD) superfamily protein	FITPB_A_wo_P, FRUITPB_A_wo_P
calcium ion transmembrane transport	12	*	AT4G03560	*TPC1*	depolarization-activated Ca(2+) channel	
calcium ion transport	12	*	AT4G03560	*TPC1*	depolarization-activated Ca(2+) channel	
regulation of salicylic acid mediated signaling pathw	10	*	AT4G03440		Ankyrin repeat family protein	FRUITSTEM_C_w_P
			AT4G03460		Ankyrin repeat family protein	GERM_A_wo_P, SILPB_B_w_P, SILPB_A_wo_P, SILSTEM_B_wo_P
			AT4G03470		Ankyrin repeat family protein	SILPB_B_w_P, SILPB_A_wo_P, SILSTEM_B_wo_P
			AT4G03500		Ankyrin repeat family protein	FRUITSTEM_C_w_P
cellular response to salicylic acid stimulus	10	*	AT4G03440		Ankyrin repeat family protein	FRUITSTEM_C_w_P
			AT4G03450		Ankyrin repeat family protein	FRUITSTEM_C_w_P, GERM_A_wo_P
			AT4G03460		Ankyrin repeat family protein	GERM_A_wo_P, SILPB_B_w_P, SILPB_A_wo_P, SILSTEM_B_wo_P
			AT4G03470		Ankyrin repeat family protein	SILPB_B_w_P, SILPB_A_wo_P, SILSTEM_B_wo_P
			AT4G03500		Ankyrin repeat family protein	FRUITSTEM_C_w_P
photosynthetic electron transport chain	10	*	AT4G03280	*PGR1*	Encodes the Rieske FeS center of cytochrome b6f complex	FRUITSTEM_C_w_P
developmental growth	7	*	AT4G03190	*AFB1*	F box protein belonging to the TIR1 subfamily	
pollen maturation	7	*	AT4G03190	*AFB1*	F box protein belonging to the TIR1 subfamily	
regulation of auxin mediated signaling pathway	5	*	AT3G59060	*PIF5*	novel Myc-related bHLH transcription factor	

*0.05 > *P* > 0.01, **0.01 > *P* > 0.001. The significance of enrichment was tested against a null distribution using 10,000 permutations.

[1] The letters A, B and C stand for the three types of soil. 'wo_P' and 'w_P' correspond to the absence and presence of *P. annua*, respectively.